# Quantification of Uncertainty in Predicting Building Energy Consumption

*a stochastic approach*

Brohus, Henrik; Frier, Christian; Heiselberg, Per; Haghighat, F.

*Published in:*
Energy and Buildings

*DOI (link to publication from Publisher):*
10.1016/j.enbuild.2012.07.013

*Publication date:*
2012

*Document Version*
Accepted author manuscript, peer reviewed version

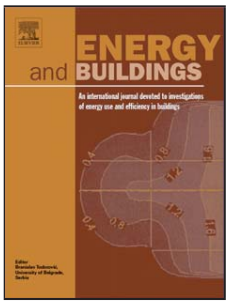


Title: Quantification of Uncertainty in Predicting Building Energy Consumption: A Stochastic Approach

Authors: H. Brohus, C. Frier, P. Heiselberg, F. Haghighat

PII: S0378-7788(12)00340-4
DOI: doi:10.1016/j.enbuild.2012.07.013
Reference: ENB 3799

To appear in: *ENB*

Received date: 24-11-2011
Revised date: 15-7-2012
Accepted date: 18-7-2012

Please cite this article as: H. Brohus, C. Frier, P. Heiselberg, F. Haghighat, Quantification of Uncertainty in Predicting Building Energy Consumption: A Stochastic Approach, *Energy and Buildings* (2010), doi:10.1016/j.enbuild.2012.07.013

# Quantification of Uncertainty in Predicting Building Energy Consumption: A Stochastic Approach

H. Brohus[1], C. Frier[1], P. Heiselberg[1] and F. Haghighat[2]
[1]Department of Civil Engineering, Aalborg University, Aalborg, Denmark (hb@civil.aau.dk)
[2]Department of Building, Civil and Environmental Engineering
Concordia University, Montreal, Quebec, Canada (haghi@cbs-engr.bcee.concordia.ca)

ABSTRACT
Traditional building energy consumption calculation methods are characterised by rough approaches providing approximate figures with high and unknown levels of uncertainty. Lack of reliable energy resources and increasing concerns about climate change call for improved predictive tools.

A new approach for the prediction of building energy consumption is presented. The approach quantifies the uncertainty of building energy consumption by means of stochastic differential equations. The approach is applied to a general heat balance for an arbitrary number of loads and zones in a building to determine the dynamic thermal response under random conditions. Two test cases are presented.

The approach is found to work well, although computation time may be rather high. The results indicate that the impact of a stochastic description compared with a deterministic description may be modest for the dynamic thermal behaviour of buildings. However, for air flow and energy consumption it is found to be much more significant due to less "damping".

Probabilistic methods establish a new approach to the prediction of building energy consumption, enabling designers to include stochastic parameters like inhabitant behaviour, operation, and maintenance to predict the performance of the systems and the level of certainty for fulfilling design requirements under random conditions.

**Keywords:** Stochastic differential equation, uncertainty quantification, building thermal behaviour, occupants' behaviour, net-zero energy buildings, building simulation tool.

**Highlights:**

- New approach to improved prediction of building energy consumption
- Quantification of uncertainty using stochastic differential equations
- Determination of the mean value process and the standard deviation process
- Probabilistic method providing uncertainty variation as a function of time

# Introduction

Traditional building energy consumption calculation methods are usually characterised by rough estimates providing only an approximate figure with high and unknown levels of uncertainty. This approach has previously been justified by low energy prices and ignorance of emission impact. However, lack of useful energy resouces and increasing concern for climate change calls for new and improved methods for the prediction of building energy consumption. This is especially important in design of new-built and refurbishment of low energy and net-zero energy buildings where there are high uncertainties in the estimation of collected energy and used energy.

The building energy consumption is influenced strongly by varying loads due to weather and occupants' behaviour. Thus, it is impossible by nature to determine a fixed number representing the exact energy consumption. In stead the energy consumption should be determined as a probability distribution or at the least as a mean value and a standard deviation. In that way the uncertainty may be quantified providing improved decision support during the design phase due to an increased and improved level of knowledge. This approach could provide a scientific base for selection of a safety factor.

Building energy simulation tool have been utilized to forecast and analyze building energy consumption and describe building energy use patterns, in order to benefit the design and operation of energy efficient buildings [1,2]. The existing simulation program such as Energy Plus, DOE-2 and BLAST consider the dynamic thermal behaviour of building to be deterministic and ignores the rapid variations in the weather conditions and other factors such as occupants' behaviour. This was mainly due to the fact that mechanically ventilated massive buildings are highly "damped" and shielded from these external and internal random loads. These types of buildings control the influence of these loads effectively by means of the BEMS (Building Energy Management System) and the HVAC system. Thus, the influence of randomness on indoor environment parameters like variation of the internal heat generation and/or infiltration on the indoor air temperature becomes quite modest.

This assumption may not be valid in the case of lighter constructions that are naturally or hybrid ventilated or in the design of nearly net energy buildings. In this case the indoor air temperature is very sensitive to the variations in loads and the building will not be able to dampen out the rapidly varying swings immediately. Accurate estimation of the performance of these buildings, nearly net zero energy buildings, become very complicated and difficult since it requires precise knowledge of the energy delivered by active solar and wind systems: it is not deterministic.

The increase in interest in design of these types of buildings, nearly zero net energy buildings or high performance building, either as new-built or retrofit, stresses the importance of developing more accurate tools that could into account fluctuation in the input parameters (weather condition, internal loads, usage, etc.). A logical approach is to use a stochastic model to describe the physical process [3,4,5]. In a stochastic model, the parameters, the input and even the initial condition are treated in stochastic term.

In a deterministic model, a numerical value, usually the mean value from various observations is specified to study the behaviour of building and indoor environment. In practise, there is always some uncertainty (randomness) associated with the specification of these parameters. Also, there are additional sources of randomness in the model specification of an appropriate

model. Representation of randomness in the model specification may be a simplification of a complex physical process such as infiltration in building load calculation. Haghighat et al. [6,7] reported the impact of fluctuating wind speed on the building change rates using spectrum analysis. They showed the effect of fluctuating infiltration is especially significant when the mean pressure differences across openings are low while their turbulent components are large. Building occupants' behaviour also significantly impacts the building energy performance. It is very difficult to deterministically represent their behaviour due to its temporal (usage of a specific appliance) or spatial (usage of a specific room) stochastic nature [8,9]. Wang et al. [10] developed a model to simulate the occupant movement process based on the Markov chain. Randomness is also present in the input to the model, for example, solar radiation, radiative and convective heat transfer coefficients, etc.

This paper reports the development a new methodology for simulating and predicting the indoor environment and energy performance of buildings. It first describes the theory of stochastic differential equations (SDE) through the application of a model to a building in order to determine the dynamic thermal behaviour under random conditions. The aim is to calculate the internal air temperature as well as the temperatures of the building structure and surface zones subject to external loads (solar gain and external temperature) and internal loads (people, lighting, equipment, etc.). Both mean values and standard deviations will be discussed. It is possible to calculate the loads and the heat losses deterministically or stochastically. Randomness both in the input (i.e, solar radiation, internal heat generation, etc.) as well as the model coefficients (i.e, convective heat transfer coefficient) is considered.

The first case study represents a conventional mechanically ventilated building with fixed heat losses between the building and the external environment and between the various building zones. The second case study is a naturally ventilated atrium, where the heat loss between the building zone and the external environment - and, thus, the air flow rate - is assumed to be driven by air density differences through the openings in the enclosure (stack effect). This case represents a simple example of a coupling between a thermal model and an air flow model. A simple probabilistic model for natural ventilation is derived, which is coupled with the SDE thermal model.

# Deterministic Building Model

The model outlined in Figure 1 comprises a general heat balance for an arbitrary number of zones, and buildings components. There are *n* nodes with an unknown temperature and *m* nodes with a known temperature; the latter are denoted boundary nodes.

For node *i* the following energy balance can be made, assuming that the heat capacity is concentrated in the nodes (lumped parameter approach), see Figure 1.

For the system of *n* equations

$$C_i \frac{d\theta_i(t)}{dt} = \sum_{\substack{j=1 \\ i \neq j}}^{n} H_{ij}(t)\left(\theta_j(t) - \theta_i(t)\right) + \sum_{j=1}^{m} H_{ij}^{b}(t)\left(\theta_j^{b}(t) - \theta_i(t)\right) + \sum_{j=1}^{k_i} \Phi_{ij}(t), \quad i = 1, 2, \ldots, n \quad (1)$$

where the first term on the right hand side represents the heat transfer between nodes with unknown temperature, the second term represents heat transfer between unknown temperature nodes and boundary nodes, and the last term is the internal heat generation.

$b$ = Boundary condition (specified temperature)
$k_i$ = Number of specified heat fluxes attached to node $i$
$m$ = Number of nodes with specified temperatures
$n$ = Number of nodes with unknown temperature
$t$ = Time (s)
$C_i$ = Effective thermal capacity of the zone representing node $i$ (J/K)
$H_{ij}$ = Specific heat loss (W/K). Due to symmetry $H_{ij} = H_{ji}$
$\theta_i$ = Temperature (°C)
$\Phi_{ij}$ = Internal heat generation (W)

The conventional approach is to consider Equation 1 as deterministic differential equation systems, which can be solved using a numerical approach. In practice the outdoor conditions and indoor parameters are random in nature: the outdoor environment (outdoor air temperature, humidity, wind speed, wind direction, solar radiation, etc.) and indoor environment (occupants behavior and activity) are random in nature suggesting that Equation 1 is a stochastic differential equation system.

# Stochastic Building Model

## Stochastic Differential Equation System

The most commonly used stochastic differential equations for continuous processes have proved to be those involving Wiener processes or Brownian motion [11]. Thus, the loads are modelled as stochastic processes each comprising a time-varying mean value function and a stochastic part described as a white noise process scaled by a time-varying standard deviation function. The close connection between the white noise process and the Wiener process is outlined in Appendix A.

**Building Model**

It is assumed that one or several of the following load variables, $\theta_j^b$, $H_{ij}$, $H_{ij}^b$ and $\Phi_{ij}$, are stochastic. Each one acts as input to the building model. The following stochastic process describes each quantity, here denoted by $z$

$$z(t) = \mu_z(t) + z'(t) = \mu_z(t) + \sigma_z(t) w_z(t) \quad (2)$$

where

$\mu_z$ = Mean value
$z'$ = Fluctuating part
$\sigma_z$ = Standard deviation
$w_z$ = White noise process

In Equation (2) the quantities are assumed to be independent. Haghighat et al. [12] discusses how to obtain stochastic load models in more detail. By insertion of equation (2) into equation (1), a system of stochastic differential equations (SDE) is established. All parameters except the heat capacity, $C_i$, are assumed functions of time, $t$.

$$\frac{d\theta_i}{dt} = \frac{1}{C_i}\sum_{\substack{j=1\\ i\neq j}}^{n}(\mu_{H_{ij}} + \sigma_{H_{ij}} w_{H_{ij}})(\theta_j - \theta_i) + \frac{1}{C_i}\sum_{j=1}^{m}(\mu_{H_{ij}^b} + \sigma_{H_{ij}^b} w_{H_{ij}^b})(\mu_{\theta_j^b} + \sigma_{\theta_j^b} w_{\theta_j^b} - \theta_i) \qquad i = 1, 2,\ldots,n$$
$$+ \frac{1}{C_i}\sum_{j=1}^{k_i}(\mu_{\Phi_{ij}} + \sigma_{\Phi_{ij}} w_{\Phi_{ij}}) \qquad (3)$$

which can be rewritten as

$$\frac{d\theta_i}{dt} = \frac{1}{C_i}\sum_{\substack{j=1\\ i\neq j}}^{n}\mu_{H_{ij}}(\theta_j - \theta_i) + \frac{1}{C_i}\sum_{j=1}^{m}\mu_{H_{ij}^b}(\mu_{\theta_j^b} - \theta_i) + \frac{1}{C_i}\sum_{j=1}^{k_i}\mu_{\Phi_{ij}}$$
$$+ \frac{1}{C_i}\sum_{\substack{j=1\\ i\neq j}}^{n}\sigma_{H_{ij}}(\theta_j - \theta_i)w_{H_{ij}} + \frac{1}{C_i}\sum_{j=1}^{m}\mu_{H_{ij}^b}\sigma_{\theta_j^b} w_{\theta_j^b} + \frac{1}{C_i}\sum_{j=1}^{m}\sigma_{H_{ij}^b}(\mu_{\theta_j^b} - \theta_i)w_{H_{ij}^b} \quad , \quad i = 1, 2, \ldots, n$$
$$+ \frac{1}{C_i}\sum_{j=1}^{m}\sigma_{H_{ij}^b}\sigma_{\theta_j^b} w_{H_{ij}^b} w_{\theta_j^b} + \frac{1}{C_i}\sum_{j=1}^{k_i}\sigma_{\Phi_{ij}} w_{\Phi_{ij}} \qquad (4)$$

Using the relationship between the white noise process, $w(t)$, and the Wiener increment, $dW(t)$ (See Appendix A), and ignoring terms in equation (4) containing $w(t)^2$, as they are insignificant compared with the other terms [12], the equation can be expressed as

$$d\theta_i = \frac{1}{C_i}\left[\sum_{\substack{j=1\\ i\neq j}}^{n}\mu_{H_{ij}}(\theta_j - \theta_i) + \sum_{j=1}^{m}\mu_{H_{ij}^b}(\mu_{\theta_j^b} - \theta_i) + \sum_{j=1}^{k_i}\mu_{\Phi_{ij}}\right]dt$$
$$+ \frac{1}{C_i}\left[\sum_{\substack{j=1\\ i\neq j}}^{n}\sigma_{H_{ij}}(\theta_j - \theta_i)dW_{H_{ij}} + \sum_{j=1}^{m}\sigma_{H_{ij}^b}(\mu_{\theta_j^b} - \theta_i)dW_{H_{ij}^b} + \sum_{j=1}^{m}\mu_{H_{ij}^b}\sigma_{\theta_j^b}dW_{\theta_j^b} + \sum_{j=1}^{k_i}\sigma_{\Phi_{ij}}dW_{\Phi_{ij}}\right]$$
$$i = 1, 2, \ldots, n \qquad (5)$$

The system of equations is linear and can be expressed as

$$d\boldsymbol{\theta} = [\mathbf{A}\boldsymbol{\theta} + \mathbf{a}]dt + \sum_{k=1}^{VAR}[\mathbf{B}^k\boldsymbol{\theta} + \mathbf{b}^k]dW_k \qquad (6)$$

where $VAR$ is the number of load variables

$$A_{ij} = \begin{cases} -\frac{1}{C_i}\left[\sum_{\substack{k=1 \\ i\neq k}}^{n} \mu_{H_{ik}} + \sum_{k=1}^{m} \mu_{H_{ik}^b}\right] & \text{for} \quad i = j \\ \frac{1}{C_i}\mu_{H_{ij}} & \text{otherwise} \end{cases} \qquad i,\ j = 1, 2, \ldots, n \tag{7}$$

$$a_i = \frac{1}{C_i}\left[\sum_{k=1}^{n} \mu_{H_{ik}^b}\mu_{\theta_k^b} + \sum_{j=1}^{k_i} \mu_{\Phi_{ij}}\right] \qquad i = 1, 2, \ldots, n \tag{8}$$

The components of the matrices, $\mathbf{B}^k$, and the vectors, $\mathbf{b}^k$, depend on the variable in question and expressions for the different variable types in equation (5) are:

For the variables $\theta_k^b$, $k = 1, 2, \ldots, m$, the following is obtained

$$B_{ij}^{\theta_k^b} = 0 \qquad i,\ j = 1, 2, \ldots, n \tag{9}$$

$$b_i^{\theta_k^b} = \frac{1}{C_i}\mu_{H_{ik}^b}\sigma_{\theta_k^b} \qquad i = 1, 2, \ldots, n \tag{10}$$

For the variables $H_{kl}$, $k = 1, 2, \ldots, l\text{-}1$, $l = 1, 2, \ldots, n$, and using that $H_{kl} = H_{lk}$, the following is obtained

$$B_{ij}^{H_{kl}} = \begin{cases} -\frac{1}{C_i}\sigma_{H_{kl}} & \text{for} \quad i = j = k \\ \frac{1}{C_i}\sigma_{H_{kl}} & \text{for} \quad i = k,\ j = l \\ \frac{1}{C_j}\sigma_{H_{kl}} & \text{for} \quad i = l,\ j = k \\ -\frac{1}{C_j}\sigma_{H_{kl}} & \text{for} \quad i = j = l \\ 0 & \text{otherwise} \end{cases} \qquad i,\ j = 1, 2, \ldots, n \tag{11}$$

$$b_i^{H_{kl}} = 0 \qquad i = 1, 2, \ldots, n \tag{12}$$

For the variables $H_{kl}^b$, $k = 1, 2, \ldots, n$, $l = 1, 2, \ldots, m$, the following is obtained

$$B_{ij}^{H_{kl}^b} = \begin{cases} -\frac{1}{C_i}\sigma_{H_{kl}^b} & \text{for} \quad i = j = k \\ 0 & \text{otherwise} \end{cases} \qquad i,\ j = 1, 2, \ldots, n \tag{13}$$

$$b_i^{H_{kl}^b} = \begin{cases} \frac{1}{C_i}\mu_{\theta_l^b}\sigma_{H_{kl}^b} & \text{for} \quad i=j=k \\ 0 & \text{otherwise} \end{cases} \qquad i,\ j = 1, 2, \dots, n \tag{14}$$

and for the variables $\Phi_{kl}$, $k = 1, 2, \dots, n$, $l = 1, 2, \dots, k_k$, the following is obtained

$$B_{ij}^{\Phi_{kl}} = 0 \qquad i,\ j = 1, 2, \dots, n \tag{15}$$

$$b_i^{\Phi_{kl}} = \begin{cases} -\frac{1}{C_i}\sigma_{\Phi_{kl}} & \text{for} \quad i=k \\ 0 & \text{otherwise} \end{cases} \qquad i,\ j = 1, 2, \dots, n \tag{16}$$

Equation (6) can also be written as

$$d\boldsymbol{\theta} = \mathbf{f}(\boldsymbol{\theta}, t)dt + \mathbf{G}(\boldsymbol{\theta}, t)d\mathbf{W} \tag{17}$$

where

$$\mathbf{f}(\boldsymbol{\theta}, t) = \mathbf{A}\boldsymbol{\theta} + \mathbf{a} \tag{18}$$

$$\mathbf{G}(\boldsymbol{\theta}, t) = [\mathbf{B}^1\boldsymbol{\theta} + \mathbf{b}^1 \quad \cdots \quad \mathbf{B}^{VAR}\boldsymbol{\theta} + \mathbf{b}^{VAR}] \tag{19}$$

$$d\mathbf{W}^{\mathrm{T}} = [dW_1 \quad \cdots \quad dW_{VAR}] \tag{20}$$

Equation (17) represents the conventional way of writing a stochastic differential equation system.

The unknown zone temperatures $\boldsymbol{\theta}$, i.e. the building model output, are not necessarily given on a form similar to equation (2) as the thermal capacities $C_i$ introduce damping into the system and, thus, time-dependence into the fluctuating part of the process. In the following two different solution techniques are outlined in order to solve equation (17).

## Moment Equation Approach

The stochastic differential equation system (17) has an infinite number of solutions, corresponding to all possible realisations of the standard Wiener processes defining the SDE. Thus, instead of directly solving (17), the statistics of the time-varying zone temperatures are obtained. The first and second-order statistical moments of the zone temperatures are derived, defining the mean value function and the covariance function respectively. These provide important information regarding the general zone temperature level and the corresponding variability, respectively.

By means of Itô's formula, see for instance [13], the following holds for a general scalar function $\varphi = \varphi(\boldsymbol{\theta}, t)$. In the following, it is implicitly assumed that **f** and **G**, given by (17), are functions of $\boldsymbol{\theta}$ and $t$.

$$d\varphi = \left[ \frac{\partial \varphi}{\partial t} + \sum_{i=1}^{n} f_i \frac{\partial \varphi}{\partial \theta_i} + \frac{1}{2} \sum_{i=1}^{n} \sum_{j=1}^{n} (\mathbf{G}\mathbf{G}^{\mathrm{T}})_{ij} \frac{\partial^2 \varphi}{\partial \theta_i \partial \theta_j} \right] dt + \frac{\partial \varphi^{\mathrm{T}}}{\partial \boldsymbol{\theta}} \mathbf{G} d\mathbf{W} \tag{21}$$

or

$$\frac{d\varphi}{dt} = \frac{\partial \varphi}{\partial t} + \sum_{i=1}^{n} f_i \frac{\partial \varphi}{\partial \theta_i} + \frac{1}{2} \sum_{i=1}^{n} \sum_{j=1}^{n} (\mathbf{G}\mathbf{G}^{\mathrm{T}})_{ij} \frac{\partial^2 \varphi}{\partial \theta_i \partial \theta_j} + \frac{\partial \varphi^{\mathrm{T}}}{\partial \boldsymbol{\theta}} \mathbf{G}\mathbf{w} \tag{22}$$

By taking the mean value one obtains

$$\frac{d\mathrm{E}[\varphi]}{dt} = \frac{\partial \mathrm{E}[\varphi]}{\partial t} + \sum_{i=1}^{n} \mathrm{E}\left[ f_i \frac{\partial \varphi}{\partial \theta_i} \right] + \frac{1}{2} \sum_{i=1}^{n} \sum_{j=1}^{n} \mathrm{E}\left[ (\mathbf{G}\mathbf{G}^{\mathrm{T}})_{ij} \frac{\partial^2 \varphi}{\partial \theta_i \partial \theta_j} \right] \tag{23}$$

Now, it is chosen that $\varphi = \prod_{i=1}^{n} \theta_i^{k_i}$, where $\sum_{i=1}^{n} k_i$ is the order of the moment for unknown temperature node, $\theta_i$.

If a building model with two unknown temperature nodes, $\theta_1$ and $\theta_2$, is considered, two first order moment equations are introduced using

$$\sum_{i=1}^{n} k_i = 1 \Rightarrow \begin{cases} (k_1 = 1, k_2 = 0) \Rightarrow \varphi = \theta_1 \\ (k_1 = 0, k_2 = 1) \Rightarrow \varphi = \theta_2 \end{cases} \tag{24}$$

Similarly, three second order equations are formulated

$$\sum_{i=1}^{n} k_i = 2 \Rightarrow \begin{cases} (k_1 = 2, k_2 = 0) \Rightarrow \varphi = \theta_1^2 \\ (k_1 = 1, k_2 = 1) \Rightarrow \varphi = \theta_1 \theta_2 \\ (k_1 = 0, k_2 = 2) \Rightarrow \varphi = \theta_2^2 \end{cases} \tag{25}$$

Moment equations can be formulated for any higher order, but this will not be considered here. Now equation (23) can be rewritten as

$$\frac{d}{dt} \mathrm{E}\left[ \prod_{s=1}^{n} \theta_s^{k_s} \right] = \sum_{i=1}^{n} \mathrm{E}\left[ f_i \frac{\partial}{\partial \theta_i} \left( \prod_{s=1}^{n} \theta_s^{k_s} \right) \right] + \frac{1}{2} \sum_{i=1}^{n} \sum_{j=1}^{n} \mathrm{E}\left[ (\mathbf{G}\mathbf{G}^{\mathrm{T}})_{ij} \frac{\partial^2}{\partial \theta_i \partial \theta_j} \left( \prod_{s=1}^{n} \theta_s^{k_s} \right) \right] \tag{26}$$

The equation for the first order moment can be found by inserting $\sum_{i=1}^{n} k_i = 1$

$$\frac{d\mathrm{E}[\boldsymbol{\theta}]}{dt} = \mathrm{E}[\mathbf{f}] = \mathrm{E}[\mathbf{A}\boldsymbol{\theta} + \mathbf{a}] \tag{27}$$

The equation for the second order moment is found by inserting $\sum_{i=1}^{n} k_i = 2$

$$\frac{d\mathrm{E}[\theta_i \theta_j]}{dt} = \mathrm{E}[\theta_i f_j] + \mathrm{E}[\theta_j f_i] + \mathrm{E}\left[(\mathbf{G}\mathbf{G}^{\mathrm{T}})_{ij}\right] \tag{28}$$

The quantity $\theta_i f_j + \theta_j f_i$ corresponds to component *i, j* in $\boldsymbol{\theta}\mathbf{f}^{\mathrm{T}} + \mathbf{f}\boldsymbol{\theta}^{\mathrm{T}}$ due to the fact that

$$\begin{aligned}\boldsymbol{\theta}\mathbf{f}^{\mathrm{T}} + \mathbf{f}\boldsymbol{\theta}^{\mathrm{T}} &= \begin{bmatrix}\theta_1 \\ \vdots \\ \theta_n\end{bmatrix}\begin{bmatrix}f_1 & \cdots & f_n\end{bmatrix} + \begin{bmatrix}f_1 \\ \vdots \\ f_n\end{bmatrix}\begin{bmatrix}\theta_1 & \cdots & \theta_n\end{bmatrix} \\ &= \begin{bmatrix}\theta_1 f_1 + f_1\theta_1 & \cdots & \theta_1 f_n + f_1\theta_n \\ \vdots & \ddots & \vdots \\ \theta_n f_1 + f_n\theta_1 & \cdots & \theta_n f_n + f_n\theta_n\end{bmatrix}\end{aligned} \tag{29}$$

Equation (27) can be rewritten as

$$\boldsymbol{\theta}\mathbf{f}^{\mathrm{T}} + \mathbf{f}\boldsymbol{\theta}^{\mathrm{T}} = \boldsymbol{\theta}[\mathbf{A}\boldsymbol{\theta} + \mathbf{a}]^{\mathrm{T}} + [\mathbf{A}\boldsymbol{\theta} + \mathbf{a}]\boldsymbol{\theta}^{\mathrm{T}} = \boldsymbol{\theta}\boldsymbol{\theta}^{\mathrm{T}}\mathbf{A}^{\mathrm{T}} + \boldsymbol{\theta}\mathbf{a}^{\mathrm{T}} + \mathbf{A}\boldsymbol{\theta}\boldsymbol{\theta}^{\mathrm{T}} + \mathbf{a}\boldsymbol{\theta}^{\mathrm{T}} \tag{30}$$

By taking the mean value one obtains

$$\mathrm{E}[\boldsymbol{\theta}\mathbf{f}^{\mathrm{T}} + \mathbf{f}\boldsymbol{\theta}^{\mathrm{T}}] = \mathrm{E}[\boldsymbol{\theta}\boldsymbol{\theta}^{\mathrm{T}}]\mathbf{A}^{\mathrm{T}} + \mathrm{E}[\boldsymbol{\theta}]\mathbf{a}^{\mathrm{T}} + \mathbf{A}\mathrm{E}[\boldsymbol{\theta}\boldsymbol{\theta}^{\mathrm{T}}] + \mathbf{a}\mathrm{E}[\boldsymbol{\theta}]^{\mathrm{T}} \tag{31}$$

$\mathbf{G}\mathbf{G}^{\mathrm{T}}$ is further examined

$$\begin{aligned}\mathbf{G}\mathbf{G}^{\mathrm{T}} &= [\mathbf{B}^1\boldsymbol{\theta} + \mathbf{b}^1 \quad \cdots \quad \mathbf{B}^{VAR}\boldsymbol{\theta} + \mathbf{b}^{VAR}][\mathbf{B}^1\boldsymbol{\theta} + \mathbf{b}^1 \quad \cdots \quad \mathbf{B}^{VAR}\boldsymbol{\theta} + \mathbf{b}^{VAR}]^{\mathrm{T}} \\ &= [\mathbf{B}^1\boldsymbol{\theta} + \mathbf{b}^1 \quad \cdots \quad \mathbf{B}^{VAR}\boldsymbol{\theta} + \mathbf{b}^{VAR}]\begin{bmatrix}(\mathbf{B}^1\boldsymbol{\theta} + \mathbf{b}^1)^{\mathrm{T}} \\ \vdots \\ (\mathbf{B}^{VAR}\boldsymbol{\theta} + \mathbf{b}^{VAR})^{\mathrm{T}}\end{bmatrix} \\ &= \sum_{k=1}^{VAR}[\mathbf{B}^k\boldsymbol{\theta} + \mathbf{b}^k][\mathbf{B}^k\boldsymbol{\theta} + \mathbf{b}^k]^{\mathrm{T}} \\ &= \sum_{k=1}^{VAR}[\mathbf{B}^k\boldsymbol{\theta} + \mathbf{b}^k][\boldsymbol{\theta}^{\mathrm{T}}(\mathbf{B}^k)^{\mathrm{T}} + (\mathbf{b}^k)^{\mathrm{T}}]^{\mathrm{T}} \\ &= \sum_{k=1}^{VAR}[\mathbf{B}^k\boldsymbol{\theta}\boldsymbol{\theta}^{\mathrm{T}}(\mathbf{B}^k)^{\mathrm{T}} + \mathbf{B}^k\boldsymbol{\theta}(\mathbf{b}^k)^{\mathrm{T}} + \mathbf{b}^k\boldsymbol{\theta}^{\mathrm{T}}(\mathbf{B}^k)^{\mathrm{T}} + \mathbf{b}^k(\mathbf{b}^k)^{\mathrm{T}}]\end{aligned} \tag{32}$$

The corresponding mean value is

$$\mathrm{E}[\mathbf{G}\mathbf{G}^{\mathrm{T}}] = \sum_{k=1}^{VAR}[\mathbf{B}^k\mathrm{E}[\boldsymbol{\theta}\boldsymbol{\theta}^{\mathrm{T}}](\mathbf{B}^k)^{\mathrm{T}} + \mathbf{B}^k\mathrm{E}[\boldsymbol{\theta}](\mathbf{b}^k)^{\mathrm{T}} + \mathbf{b}^k\mathrm{E}[\boldsymbol{\theta}]^{\mathrm{T}}(\mathbf{B}^k)^{\mathrm{T}} + \mathbf{b}^k(\mathbf{b}^k)^{\mathrm{T}}] \tag{33}$$

By considering (27) and by inserting (31) and (33) into (27) the following deterministic differential equations for the first and second order moments of $\boldsymbol{\theta}$ can be determined [13]

$$\begin{cases} \dfrac{d\mathrm{E}[\boldsymbol{\theta}]}{dt} = \mathbf{A}\mathrm{E}[\boldsymbol{\theta}] + \mathbf{a} \\ \textit{with initial conditions} \\ \mathrm{E}[\boldsymbol{\theta}(t = t_0)] = \mathrm{E}[\boldsymbol{\theta}^0] \end{cases} \tag{34}$$

$$\begin{cases} \dfrac{d\mathrm{E}[\boldsymbol{\theta}\boldsymbol{\theta}^{\mathrm{T}}]}{dt} = \mathbf{A}\mathrm{E}[\boldsymbol{\theta}\boldsymbol{\theta}^{\mathrm{T}}] + \mathrm{E}[\boldsymbol{\theta}\boldsymbol{\theta}^{\mathrm{T}}]\mathbf{A}^{\mathrm{T}} + \mathbf{a}\mathrm{E}[\boldsymbol{\theta}]^{\mathrm{T}} + \mathrm{E}[\boldsymbol{\theta}]\mathbf{a}^{\mathrm{T}} \\ + \sum_{k=1}^{VAR}[\mathbf{B}^k\mathrm{E}[\boldsymbol{\theta}\boldsymbol{\theta}^{\mathrm{T}}](\mathbf{B}^k)^{\mathrm{T}} + \mathbf{B}^k\mathrm{E}[\boldsymbol{\theta}](\mathbf{b}^k)^{\mathrm{T}} + \mathbf{b}^k\mathrm{E}[\boldsymbol{\theta}]^{\mathrm{T}}(\mathbf{B}^k)^{\mathrm{T}} + \mathbf{b}^k(\mathbf{b}^k)^{\mathrm{T}}] \\ \textit{with initial conditions} \\ \mathrm{E}[\boldsymbol{\theta}(t = t_0)\boldsymbol{\theta}(t = t_0)^{\mathrm{T}}] = \mathrm{E}[\boldsymbol{\theta}^0(\boldsymbol{\theta}^0)^{\mathrm{T}}] \end{cases} \tag{35}$$

In this way, the stochastic equations are turned into deterministic equations. Instead of an instantaneous value, the solution provides statistical quantities, i.e. first and second-order statistical moments. The first-order statistical moments correspond to the mean value of the unknown node temperatures, corresponding to a deterministic calculation, whereas the second-order equations include the variability. The conventional numerical techniques could be used to solve the system of ordinary differential equations.

## Monte Carlo Simulation Approach

The alternative approach of Monte Carlo Simulation uses realisations of the stochastic input processes generated according to their joint density functions. The corresponding output is then calculated from a deterministic model, which expresses the response of the building model. If the procedure is repeated a large number of times the resulting output data can be treated statistically.

In order to solve for a realisation of a stochastic linear differential equation a stochastic version of the fourth-order Runge-Kutta method is available [14]. Figure 2 shows the principle for calculating $\boldsymbol{\theta}_{n+1}$ using four calculation points within the time step.

The time series is divided into a number of equal time increments. The Runge-Kutta method then propagates the solution of the zone temperatures by

$$\boldsymbol{\theta}_{n+1} = \boldsymbol{\theta}_n + \frac{1}{6}\left[(\mathbf{f}_0 + 2\mathbf{f}_1 + 2\mathbf{f}_2 + \mathbf{f}_3)h + (\mathbf{G}_0 + 2\mathbf{G}_1 + 2\mathbf{G}_2 + \mathbf{G}_3)\Delta\mathbf{W}_{n+1}\right] \tag{36}$$

where

$$\mathbf{f}_0 = \mathbf{f}(\boldsymbol{\theta}_n, t_n) \tag{37}$$

$$\mathbf{G}_0 = \mathbf{G}(\boldsymbol{\theta}_n, t_n) \tag{38}$$

$$\mathbf{f}_i = \mathbf{f}\left(\boldsymbol{\theta}_n + \tfrac{1}{2}\mathbf{f}_{i-1}h + \tfrac{1}{2}\mathbf{G}_{i-1}\Delta\mathbf{W}_{n+1}\,,\, t_n + \tfrac{1}{2}h\right) \quad i = 1, \ldots, 3 \tag{39}$$

$$\mathbf{G}_i = \mathbf{G}\left(\boldsymbol{\theta}_n + \tfrac{1}{2}\mathbf{f}_{i-1}h + \tfrac{1}{2}\mathbf{G}_{i-1}\Delta\mathbf{W}_{n+1}\,,\, t_n + \tfrac{1}{2}h\right) \quad i = 1, \ldots, 3 \tag{40}$$

$$\Delta\mathbf{W}_{n+1} = \mathbf{W}_{n+1} - \mathbf{W}_n \tag{41}$$

$$h = t_{n+1} - t_n = \Delta t_{n+1} \tag{42}$$

The Wiener process increment, $\Delta\mathbf{W}_{n+1}$, is drawn from a normal distribution, N(0, $\sqrt{\Delta t_{n+1}}$).

A realisation of the solution process can be generated by means of equation (36). These equations are also applied in the solution of the two statistical moment equations (34) and (35). In that case, $\Delta\mathbf{W}_{n+1}$ is replaced by the zero vector and **f** is replaced with the right hand side of equations (34) and (35).

# Results

Two case studies have been chosen in order to demonstrate and evaluate the method, and to investigate the influence of inclusion of the stochastic elements in the differential equations that govern the problem.

The first test case comprises office rooms in a typical mechanically ventilated building exposed to internal and external loads. It has been chosen to focus on a design load period of one warm week during summer. The second test case is a naturally ventilated atrium, where the heat loss between the atrium and the external environment is stack (temperature) driven. A simple probabilistic model for stack-driven natural ventilation is presented and coupled with the SDE approach enabling the determination of the time-varying mean and standard deviation of the specific heat loss.

## Case Study 1

Figure 3 shows the first case study which comprises a two-zone building, e.g. an office building. Each zone may represent either one single room or a number of closely related rooms in proper contact. The number of unknown temperatures is six.

In theory, the number of zones (unknown temperatures) may be increased arbitrarily depending on the objectives of simulation, computer power and stability of the numerical solution of an increasingly large number of differential equations. As an example, it should be noted that when the statistical moments are determined, the number of differential equations is 27 in this case; six for the first moment and 21 for the second moment.

For each zone, three unknown temperatures are to be determined (internal air, surface layer, and structure), i.e. $\theta_1$ - $\theta_3$ for Zone I and $\theta_4$ - $\theta_6$ for Zone II. By means of the specific heat loss coefficient between Zone I and Zone II, $H_{14}$, mutual energy exchange between the zones is allowed. This could be due to transmission heat loss as well as ventilation heat loss.

The thermal capacity of each zone is selected corresponding to a medium-weight building. The ventilation corresponds to an air change rate of approximately 3 $h^{-1}$ expressed in terms of $H_{vent}$.

The two main zones are surrounded by three adjacent zones A, B, and C, where C is shared. The mean temperature and the standard deviation for the three adjacent zones are given in Table B-1 in Appendix B. The simulations are performed for a warm week in mid-August. Load profiles are employed based on the Danish Design Reference Year (DRY) [15].

In the simulation, two 24-hour load profiles – one for each zone - for the mean value of the internal sensible heat load are applied as step profiles. The sensible heat is divided into 50% convective heat, $\Phi_{conv}$, supplied to the internal air nodes, and 50% radiative heat, $\Phi_{rad}$, supplied to the surface layer nodes. The standard deviation of the internal load is assumed to be 0.3-times the mean value as a rough estimate. The 24-hour internal load profiles are repeated when the simulation exceeds 24 hours. Appendix B shows the mean value and the 95% confidence interval for the outdoor temperature, internal load and solar radiation. It also provides input parameters used for this case study, See Table B-1, as well as initial values.
The covariance, $\mathrm{Cov}_{\theta_i\theta_j}$, and thereby the standard deviation of the parameters are then equal to zero as

$$\mathrm{Cov}_{\theta_i\theta_j} = \mathrm{E}[\theta_i\,\theta_j] - \mathrm{E}[\theta_i]\mathrm{E}[\theta_j] \tag{44}$$

Figure 4 shows results from the deterministic solution for the two internal air temperatures, $\theta_1$ and $\theta_4$.

If the two curves in Figure 4 are compared, it is found that the highest temperatures occur in Zone II, where the facade faces south and the internal heat load is the highest, see Figures in Appendix B. Another interesting point is that the two zones achieve almost periodic stationary conditions after approximately 2 – 3 days.

Figure 5 shows the mean value process for the internal air and the wall surface temperature of Zone I. In addition the 95% confidence interval is shown corresponding to ±1.96 times the standard deviation process. The standard deviation is derived by solving equations (34) and (35) simultaneously.

Figure 6 shows three realisations of the stochastic process together with the 95% confidence interval for the same temperatures as in Figure 5. Only 5.5 hours of the entire week is presented in order to show the stochastic fluctuations as clearly as possible.

If the confidence intervals of the two temperatures are compared it is found that their sizes are of the same order of magnitude. However, if the fluctuations are observed it is easily seen that the overall stochastic behaviour of the two temperatures differ. The internal air temperature, $\theta_1$, obviously fluctuates rapidly, whereas the surface layer temperature, $\theta_2$, behaves more damped. Expressed in statistical terms, the autocorrelation of $\theta_2$ is higher than the autocorrelation of $\theta$, which corresponds very well with the physics of the problem. This message is not conveyed by the statistical moment approach, where only the mean value and the standard deviation are calculated.

The moment approach can be expanded to include third-order moments (in theory arbitrarily high orders are possible) in which case the skewness as a function of time is included [12]. However, this approach is extremely expensive in computer power and it still lacks information about the autocorrelation.

Monte Carlo Simulation, i.e. statistical treatment of a very high number of realisations as illustrated in Figure 6, is another promising way to obtain further information of the output processes, among others skewness, kurtosis, and autocorrelation.

## Case Study 2

**Description of case study**

This case study comprises a naturally ventilated atrium surrounded by building parts exposed to internal and external loads, see Figure 7. The thermal capacity of the atrium corresponds to a medium-weight building. The atrium is naturally ventilated with two equally sized openings without control.

The calculations are performed for a warm week in summer (Aug 15 – 21) and for a cold week in winter (Feb 15 – 21), which can be thought of as a kind of design load periods. The simulations are started three days earlier in order to avoid unrealistic values due to the initial guess. The external air temperature and the direct and diffuse solar radiation are modelled using the probabilistic models given in Brohus et al. [16].

An assumed 24-hour load profile for the mean value of the internal sensible heat load is applied in the simulation as shown in figure C-1 (see Appendix C). This appendix also provides information for the other input parameters. The sensible heat is divided into 50% convective heat, $\Phi_{conv}$, and 50% radiative heat, $\Phi_{rad}$. The convective heat flow is assumed to influence the internal air, i.e. $\theta_1$, and the radiative heat flow is assumed to influence the surface layer, i.e. $\theta_2$.

In equation (1) some of the specific heat losses, $H$, account for the ventilation heat loss. In the previous work this parameter has been assumed - and in practice prescribed as a fixed mean value and standard deviation. Now, this approach is expanded by coupling the thermal model to a simple air flow model for natural ventilation.

**Natural ventilation heat loss**

The heat loss due to ventilation, $H_{vent}$, can be estimated by (See Appendix D):

$$H_{vent} = \rho c_p C_D A (g\Delta h)^{1/2} \left[ \frac{\theta_1 - \theta_{ext}}{\theta_{ext} + 273.15} \right]^{1/2} \tag{45}$$

If the $[(\theta_1 - \theta_{ext})/(\theta_{ext} + 273.15)]^{1/2}$ term in equation (50) is introduced directly in equation (1) the system of differential equations becomes nonlinear in $\theta$ and cannot be solved by means of the techniques as described earlier. In order to avoid nonlinearity, the values of $\theta_1$ and $\theta_{ext}$ are adapted throughout the simulations from the previous time step. Thus, the air flow

model and the thermal model must be coupled. $H_{vent}$ is found by assuming a constant value for the term $\rho c_p C_D A(g\Delta h)^{1/2} = 6 \cdot 10^4$ W/K during the simulations.

**Taylor series expansion**

The heat loss due to natural ventilation, $H_{vent}$, must be modelled as a time-varying stochastic process in order to use the model, equation (45), together with the SDE approach. The deterministic part of $H_{vent}$ is modelled by a time-varying mean value function, $\mu_{H_{vent}}$, and a time-varying standard deviation function, $\sigma_{H_{vent}}$, is used to represent the fluctuating part. It is observed, that $H_{vent}$ is a nonlinear function of the temperatures, $\theta_1$ and $\theta_{ext}$, which can be regarded as input quantities, whose statistics, $\mu_{\theta_1}$, $\sigma_{\theta_1}$, $\mu_{\theta_{ext}}$ and $\sigma_{\theta_{ext}}$, at a given time, are available from the previous time step.

In order to obtain an approximation of the requested statistics, a first-order Taylor series expansion of $H_{vent}$ based on the mean value vector, $\boldsymbol{\mu} = [\,\mu_{\theta_1} \;\; \mu_{\theta_{ext}}\,]^T$, is conducted.

$$H_{vent}(\theta_1, \theta_{ext}) \approx H_{vent}(\boldsymbol{\mu}) + \left.\frac{dH_{vent}}{d\theta_1}\right|_{\boldsymbol{\mu}} (\theta_1 - \mu_{\theta_1}) + \left.\frac{dH_{vent}}{d\theta_{ext}}\right|_{\boldsymbol{\mu}} (\theta_{ext} - \mu_{\theta_{ext}}) \tag{46}$$

The mean value, $\mu_{H_{vent}}$, and the standard deviation, $\sigma_{H_{vent}}$, are obtained by conducting mean value and variance operations on the linearised equation (45) [17]

$$\begin{aligned}
\mu_{H_{vent}} &= \mathrm{E}[H_{vent}(\theta_1, \theta_{ext})] \\
&\approx \mathrm{E}\left[ H_{vent}(\boldsymbol{\mu}) + \left.\frac{dH_{vent}}{d\theta_1}\right|_{\boldsymbol{\mu}} (\theta_1 - \mu_{\theta_1}) + \left.\frac{dH_{vent}}{d\theta_{ext}}\right|_{\boldsymbol{\mu}} (\theta_{ext} - \mu_{\theta_{ext}}) \right] \\
&= H_{vent}(\boldsymbol{\mu})
\end{aligned} \tag{47}$$

$$\begin{aligned}
\sigma^2_{H_{vent}} &= \mathrm{E}\left[ \left( H_{vent}(\theta_1, \theta_{ext}) - H_{vent}(\boldsymbol{\mu}) \right)^2 \right] \\
&\approx \mathrm{E}\left[ \left( \left.\frac{dH_{vent}}{d\theta_1}\right|_{\boldsymbol{\mu}} (\theta_1 - \mu_{\theta_1}) + \left.\frac{dH_{vent}}{d\theta_{ext}}\right|_{\boldsymbol{\mu}} (\theta_{ext} - \mu_{\theta_{ext}}) \right)^2 \right] \\
&= \left[ \left.\frac{dH_{vent}}{d\theta_1}\right|_{\boldsymbol{\mu}} \;\; \left.\frac{dH_{vent}}{d\theta_{ext}}\right|_{\boldsymbol{\mu}} \right] \begin{bmatrix} \mathrm{E}[(\theta_1 - \mu_{\theta_1})^2] & \mathrm{E}[(\theta_1 - \mu_{\theta_1})(\theta_{ext} - \mu_{\theta_{ext}})] \\ \mathrm{E}[(\theta_{ext} - \mu_{\theta_{ext}})(\theta_1 - \mu_{\theta_1})] & \mathrm{E}[(\theta_{ext} - \mu_{\theta_{ext}})^2] \end{bmatrix} \begin{bmatrix} \left.\frac{dH_{vent}}{d\theta_1}\right|_{\boldsymbol{\mu}} \\ \left.\frac{dH_{vent}}{d\theta_{ext}}\right|_{\boldsymbol{\mu}} \end{bmatrix} \\
&= \left[ \left.\frac{dH_{vent}}{d\theta_1}\right|_{\boldsymbol{\mu}} \;\; \left.\frac{dH_{vent}}{d\theta_{ext}}\right|_{\boldsymbol{\mu}} \right] \mathbf{Cov}_{\boldsymbol{\theta\theta}} \begin{bmatrix} \left.\frac{dH_{vent}}{d\theta_1}\right|_{\boldsymbol{\mu}} \\ \left.\frac{dH_{vent}}{d\theta_{ext}}\right|_{\boldsymbol{\mu}} \end{bmatrix}
\end{aligned} \tag{48}$$

where $\mathbf{Cov_{\theta\theta}}$ is the covariance matrix of the vector, $\boldsymbol{\theta} = [\theta_1 \ \ \theta_{ext}]^T$.

By assuming zero correlation between $\theta_1$ and $\theta_{ext}$, the covariance matrix is a diagonal matrix with the variances of the input processes in the diagonal, and the following expression is obtained (admittedly, this is a crude assumption which is, however, necessary to avoid considering a rather complex correlation between input and output parameters in the present model)

$$\sigma_{H_{vent}}^2 \approx \sigma_{\theta_1}^2 \left.\frac{dH_{vent}}{d\theta_1}\right|_{\boldsymbol{\mu}}^2 + \sigma_{\theta_{ext}}^2 \left.\frac{dH_{vent}}{d\theta_{ext}}\right|_{\boldsymbol{\mu}}^2 \tag{49}$$

Thus, the derivatives of equation (45) with respect to the temperatures, $\theta_1$ and $\theta_{ext}$, must be obtained in order to calculate the variance of the specific heat loss due to natural ventilation.

$H_{vent}$ can also be written as

$$H_{vent} = \rho c_p C_D A (g\Delta h)^{1/2} \left[\frac{\Theta_1 - \Theta_{ext}}{\Theta_{ext}}\right]^{1/2} = const \left[\frac{\Theta_1 - \Theta_{ext}}{\Theta_{ext}}\right]^{1/2} \tag{50}$$

where $\Theta_i = \theta_i + 273.15$ is the absolute temperature and *const* is a constant value.

The derivative of $H_{vent}$ with respect to $\theta_1$ is then

$$\frac{dH_{vent}}{d\theta_1} = \frac{dH_{vent}}{d\Theta_1}\frac{d\Theta_1}{d\theta_1} = \frac{const}{2}\left[\frac{\Theta_1 - \Theta_{ext}}{\Theta_{ext}}\right]^{-1/2}\left(\frac{1}{\Theta_{ext}}\right) = \frac{const}{2\sqrt{\Theta_1\Theta_{ext} - \Theta_{ext}^2}} \tag{51}$$

The derivative of $H_{vent}$ with respect to $\theta_{ext}$ is

$$\frac{dH_{vent}}{d\theta_{ext}} = \frac{dH_{vent}}{d\Theta_{ext}}\frac{d\Theta_{ext}}{d\theta_{ext}} = \frac{const}{2}\left[\frac{\Theta_1 - \Theta_{ext}}{\Theta_1}\right]^{-1/2}\left(\frac{-\Theta_1}{\Theta_{ext}^2}\right) = \frac{-const\cdot\Theta_1}{2\sqrt{\Theta_1\Theta_{ext}^3 - \Theta_{ext}^4}} \tag{52}$$

Thus, the mean value and the standard deviation of $H_{vent}$ are obtained by inserting the equations (51) – (52) into the equations (47) and (48).

**Coupling of thermal models and air flow models**

Heat transfer and airflow in buildings are closely related physical processes, which are strongly coupled according to the Navier-Stokes equations and the energy equation. In order to obtain a solution it is necessary to solve the entire set of partial differential equations, for instance, by means of Computational Fluid Dynamics. This approach, however, is rather cumbersome and at present is too expensive in terms of computer power if long-term dynamic simulations are needed.

Therefore, modellers most often treat heat transfer and mass transfer separately in order to create simpler and easy-to-use formulas. When the interaction between heat and mass transfer is to be considered various kinds of methods for coupling can be applied, see Figure 8.

The most simple and basic model for coupling of thermal and air flow models is the so-called sequential coupling [18]. As indicated in the figure, the air flow rates are calculated with assumed temperatures first. Then the result is applied in the heat transfer model without any feedback.

Feedback between the models is used in the two other coupling methods “ping-pong” and “onions”. In case of “ping-pong”, the feedback from the heat transfer models is fed into the air flow models for the next time step. The “onions” coupling method uses mutual feedback until convergence is reached for each time step. In case of sequential coupling and “ping-pong” it is possible to reverse the coupling, in which case the heat balance is calculated in advance of the mass balance.

The choice of method depends on the required accuracy. “Onions” is the most computationally expensive method, but at the same time, the most accurate one. “Ping-pong” should be applied with care if the time steps are long and the physical coupling is strong [19].

**Results**

Figure 9 shows the mean value process for the internal air during the winter week (left) and during the summer week (right). In addition the 95% confidence interval is shown corresponding to the mean value process ±1.96 times the standard deviation process. Due to a considerable air change rate, see Figure 10, the internal temperature is only slightly higher than the external air temperature, e.g. 3–6 °C.

In this paper, the SDE approach is applied on a heat balance in order to examine the thermal behaviour of a relatively heavy building. However, if the approach is applied on a mass balance in order to determine for instance the contaminant concentration in a relatively light and hybrid or naturally ventilated building it is expected that randomness would play a more significant role.

# Conclusions

A new approach to the prediction of building energy consumption is presented. The approach quantifies the uncertainty of building energy consumption by means of stochastic differential equations (SDE). The SDE approach is applied to a general heat balance for an arbitrary number of loads and zones in a building to determine the dynamic thermal response under random conditions. Randomness in input as well as in the model coefficients (specific heat losses) is considered.

Two test cases are presented comprising a mechanically ventilated office building (case 1) and a naturally ventilated atrium (case 2). Solar radiation and external air temperature are applied as external loads. Stepwise sensible heat load profiles, divided into radiative and convective heat flow, are used as internal loads. For test case 1, all specific heat losses are prescribed in advance.

In test case 2, the specific heat loss between the atrium and the external environment is related to stack-driven natural ventilation and is thus a function of the temperature difference between the building and the environment. Thus, an air flow model is coupled with the thermal model in order to also include the influence of natural ventilation on the dynamic thermal behaviour. The "ping-pong" coupling method is applied based on a Taylor series expansion approach.

The approach is found to work well, although the computation time is rather high (several hours on an Athlon 1 GHz PC). However, there are several possibilities for reducing the computation time. A simulation of an entire year may take more than a week.

The results indicate that the impact of a stochastic description compared with a deterministic description may be modest for the dynamic thermal behaviour of buildings. However, for air flow and energy consumption it is expected that consideration of randomness will be much more significant due to less "damping" in the governing equations.

One important future improvement of the SDE approach is to improve the description of the loads. Inclusion of wind (in the model for natural ventilation) would be a very important step forward. The internal load could be improved, for example, by means of a model for window opening in the form of a distribution function.

In order to be able to use the white noise assumption, which is applied in the SDE approach, the fluctuating parts of the processes are assumed independent with respect to both mutual correlation and individual correlation in time, i.e. auto correlation. In reality, the processes will to some extent be correlated both in time and mutually. Future modelling may include auto correlation functions, describing the time-dependence of the parameters, and cross correlation functions, describing the mutual dependence.

Probabilistic methods establish a new approach to the prediction of building energy consumption, which, apart from more realistic modelling, enable designers to include stochastic parameters like inhabitant behaviour, operation, and maintenance to predict the performance of the systems and the level of certainty for fulfilling design requirements under random conditions.

# References

[1] T. Reddy, Agami, Literature Review on Calibration of Building Energy Simulation Programs: Uses, Problems, Procedures, Uncertainty, and Tools, ASHRAE Transactions 112/1 (2006) 226-240.

[2] Z. Yu, F. Haghighat, B.C.M. Fung, H. Yoshino, A decision tree method for building energy demand modeling", Energy and Buildings, 42 (2010) 1637-1646.

[3] K. Pietrzyk, Thermal Performance of a Building Envelope -- A Probabilistic Approach. Journal of Building Physics, 34/1 (2010) 77-96.

[4] J. Page, D. Robinson, N. Morel,, J.-L. Scartezzini, A generalised stochastic model for the simulation of occupant presence, Energy & Buildings, 40/2 (2008) 83-98.

[5] G.Y. Yun, P. Tuohy, K. Steemers, Thermal performance of a naturally ventilated building using a combined algorithm of probabilistic occupant behaviour and deterministic heat and mass balance models. Energy and Buildings 41/5 (2009) 489-499.

[6] F. Haghighat, J. Rao, P. Fazio, The Influence of Turbulent Wind on Air Change-Rates – A Modeling Approach, Building and Environment, 26/2 (1991) 95-109.

[7] F. Haghighat, H. Brohus, J. Rao, Modelling Air Infiltration due to Wind Fluctuations - A Review, Building and Environment 35 (2000) 377-385.

[8] H.O. Rijal, P. Tuohy, Humphreys, J.F. Nicol, A. Zamuel, An algorithm to represent occupant use of windows and fans including situation-specific motivations and constraints. Building Simulation 4/2 (2011) 117-134.

[9] Y. Jian, Y. Guo, J. Liu, Z. Bai, Q. Li, Case study of window opening behaviour using field measurement results, Building Simulation, 4/2 (2011) 107-116.

[10] C. Wang, Y. Da, J. Yi, A novel approach for building occupancy simulation, Building Simulation, 4/2 (2011) 149-167.

[11] H.C. Tuckwell, Elementary Applications of Probability Theory, with an introduction to stochastic differential equations, Second edition, ISBN 0 412 57620 1, Chapman & Hall, 1995.

[12] F. Haghighat, M. Chandrashekar, T.E. Unny, Thermal Behaviour of Buildings under Random Conditions, Applied Mathematical Modelling, 11/5 (1987) 349-356.

[13] L. Arnold, Stochastic Differential Equations, Theory and Applications, John Wiley & Sons, 1977.

[14] T.C. Gard, Introduction to Stochastic Differential Equations, ISBN 0-8247-7776-X, Marcel Dekker, New York, 1998.

[15] J.M. Jensen, H. Lund, Design Reference Year, DRY - et nyt dansk referenceår, Meddelelse Nr. 281, Laboratoriet for Varmeisolering, ISSN 1395-0266, Technical University of Denmark, Lyngby, Denmark (In Danish), 1995.

[16] H. Brohus, C. Frier, P. Heiselberg, Stochastic Load Models based on Weather Data, Annex 35 Technical Report TR17, Department of Building Technology and Structural Engineering, Aalborg University, DK-9000 Aalborg, Denmark, 2002.

[17] S.M. Ross, Introduction to probability and statistics for engineers and scientists, John Wiley & Sons, ISBN 0471608157, 1987.

[18] J. Kendrick, An Overview of Combined Modelling of Heat Transport and Air Movement, ISBN 0 946075 70 0, AIC-TN-40-1993, Air Infiltration and Ventilation Centre, Coventry, Great Britain, 1993.

[19] M. Orme, Applicable Models for Air Infiltration and Ventilation Calculations, AIC-TN-51-1999, ISBN 1 902177 09 6, AIVC, Coventry, Great Britain, 1999.

[20] CIBSE, Natural Ventilation in Non-domestic Buildings, Applications Manual AM10:1997, CIBSE, London, 1997.

[21] P.L. Olufsen, Trykforhold i bygninger, Chapter 15, In: H.E. Hansen, P. Kjerulf-Jensen, O.B. Stampe, Varme- og Klimateknik, Grundbog, 2. udgave, ISBN 87-98-2652-8-8, Danvak ApS, Denmark (In Danish), 1997.

# Appendix A

**Wiener Processes, white noise, stochastic differential equation and Itô's formula**

A standard Wiener process $W = \{W(t), t > 0\}$ on [0,T], is a process with stationary independent increments such that for any $0 \le t_1 \le t_2 \le T$, the increment $W(t_2) - W(t_1)$ is a Gaussian (i.e. normally distributed) random variable with zero mean and variance equal to $t_2 - t_1$, see [14]; i.e.

$$\mathrm{E}[W(t_2) - W(t_1)] = E[\Delta W] = 0 \tag{A.1}$$

$$\mathrm{Var}[W(t_2) - W(t_1)] = Var[\Delta W] = t_2 - t_1 = \Delta t \tag{A.2}$$

$$\mathrm{P}[W(0) = 0] = 1 \tag{A.3}$$

Then the following holds for two independent Wiener processes, $W_i$ and $W_j$, with infinitesimal increments, $dW_i$ and $dW_j$:

$$\begin{aligned} E[dW_i\, dW_j] &= 0 \quad , \quad i \neq j \\ E[dW_i^2] &= dt \quad , \quad i = j \end{aligned} \tag{A.4}$$

As a Gaussian process, the Wiener process has the important feature that the two first moments, i.e. the mean and the covariance, completely define the probability law.

The autocovariance function of a standard Wiener process is

$$\mathrm{Cov}_{\mathrm{WW}}(s,t) = \min(s,t) \tag{A.5}$$

where min(.,.) is defined as the smallest value of the two arguments.

The Wiener process belongs to a class of processes whose behaviour during any time interval is independent of their behaviour during any non-overlapping time interval. Thus the evolution of the process after any time $\tau > 0$ is independent of the time history up to and including $\tau$. The properties of a Wiener process are that $W(0) = 0$, the mean value at any time is zero, and that the variances increases with $t$. Figure A.1 sketches two realisations of a standard Wiener process.

Gaussian white noise is a very important concept in the theory of stochastic differential equations. Although the derivative of the so-called Wiener process does not exist, it is often heuristically convenient to assume that it actually does [14]. The symbol $w$(t) is used for this "derivative" denoted white noise and $w = \{w(t), t \ge 0\}$ on [0, $T$].

$$w(t)dt = dW(t) \tag{A.6}$$

The moments of a white noise process are derived from the Wiener process [11]:

$$\mathrm{E}[w(t)] = 0 \tag{A.7}$$

$$\mathrm{Cov}_{\mathrm{ww}}(s,t) = \delta(t-s) \tag{A.8}$$

where $\delta(a)$ is Dirac's delta function, thus $\delta(\mathrm{a}) = 0$ ($\mathrm{a} \neq 0$) and $\delta(0) = +\infty$, and

$$\int_{-\infty}^{\infty} \delta(a)da = 1 \tag{A.9}$$

A linear first order stochastic differential equation involving $n$ output variables, $\theta_i$ , $i = 1,\ldots,n$, and input properties defined by $m$ Wiener processes, $dW_k$ , $k = 1,\ldots,m$ can be written as in (17):

$$d\boldsymbol{\theta} = \mathbf{f}(\boldsymbol{\theta},t)dt + \mathbf{G}(\boldsymbol{\theta},t)\mathbf{dW} \tag{A.10}$$

In the following, it is implicitly assumed that **f** and **G**, given by (A.10), are functions of $\boldsymbol{\theta}$ and $t$, which can then be written in component form as:

$$d\theta_i = f_i\, dt + \sum_{k=1}^{m} g_{ik}\, dW_k \tag{A.11}$$

By means of Itô's formula, see for instance [13], the following holds for a general scalar function $\varphi = \varphi(\boldsymbol{\theta},t)$:

$$d\varphi = \left[\frac{\partial\varphi}{\partial t} + \sum_{i=1}^{n} f_i \frac{\partial\varphi}{\partial\theta_i} + \frac{1}{2}\sum_{i=1}^{n}\sum_{j=1}^{n}(\mathbf{G}\mathbf{G}^{\mathrm{T}})_{ij}\frac{\partial^2\varphi}{\partial\theta_i\partial\theta_j}\right]dt + \frac{\partial\varphi^{\mathrm{T}}}{\partial\boldsymbol{\theta}}\mathbf{G}d\mathbf{W} \tag{A.12}$$

A formal proof of Itô's formula can be found in [14]. An heuristic explanation goes as follows. By applying a second order Taylor series expansion of the scalar function, the following is obtained:

$$d\varphi = \frac{\partial\varphi}{\partial t}dt + \sum_{i=1}^{n}\frac{\partial\varphi}{\partial\theta_i}d\theta_i + \frac{1}{2}\frac{\partial^2\varphi}{\partial t^2}dt^2 + \frac{1}{2}\sum_{i=1}^{n}\frac{\partial^2\varphi}{\partial\theta_i\partial t}d\theta_i dt + \frac{1}{2}\sum_{i,j=1}^{n}\frac{\partial^2\varphi}{\partial\theta_i\partial\theta_j}d\theta_i d\theta_j \tag{A.13}$$

When expressing deterministic differential equations, only first order variations are considered, as the second order terms vanish, as $d\theta_i \to 0$ and $dt \to 0$, and the differential equation would only consist of the first two terms.

However, when $d\theta_i$ and $d\theta_j$ are substituted in (A.13) with the stochastic differential equation (A.11), then it turns out that terms involving $(d\theta_i)^2$ may not be disregarded when setting up the differential as $dW_k^2$ acts as $dt$ due to (A.4) and thus only the second and third terms in (A.13) vanish:

$$
\begin{aligned}
d\varphi &= \frac{\partial \varphi}{\partial t} dt + \sum_{i=1}^{n} \frac{\partial \varphi}{\partial \theta_i} d\theta_i + \frac{1}{2} \sum_{i,j=1}^{n} \frac{\partial^2 \varphi}{\partial \theta_i \partial \theta_j} d\theta_i d\theta_j \\
&= \frac{\partial \varphi}{\partial t} dt + \sum_{i=1}^{n} \frac{\partial \varphi}{\partial \theta_i} \left[ f_i \, dt + \sum_{k=1}^{m} g_{ik} \, dW_k \right] + \\
&\quad \frac{1}{2} \sum_{i,j=1}^{n} \frac{\partial^2 \varphi}{\partial \theta_i \partial \theta_j} \left[ f_i \, dt + \sum_{k=1}^{m} g_{ik} dW_k \right] \left[ f_j \, dt + \sum_{l=1}^{m} g_{jl} \, dW_l \right]
\end{aligned}
\tag{A.14}
$$

Terms involving $dW_i \, dW_j$ and $dt^2$ but not $dW_i^2$ can be excluded, leading to Itô's formula :

$$
\begin{aligned}
d\varphi &= \frac{\partial \varphi}{\partial t} dt + \sum_{i=1}^{n} \frac{\partial \varphi}{\partial \theta_i} \left[ f_i(\boldsymbol{\theta}, t) dt + \sum_{k=1}^{m} g_{ik}(\boldsymbol{\theta}, t) dW_k \right] + \frac{1}{2} \sum_{i,j=1}^{n} \frac{\partial^2 \varphi}{\partial \theta_i \partial \theta_j} \left[ \sum_{k=1}^{m} g_{ik} \, dW_k^2 \right] \\
&= \left[ \frac{\partial \varphi}{\partial t} + \sum_{i=1}^{n} f_i \frac{\partial \varphi}{\partial \theta_i} + \frac{1}{2} \sum_{i,j=1}^{n} \frac{\partial^2 \varphi}{\partial \theta_i \partial \theta_j} \sum_{k=1}^{m} g_i^k g_j^k \right] dt + \sum_{i=1}^{n} \frac{\partial \varphi}{\partial \theta_i} \sum_{k=1}^{m} g_{ik} dW_k
\end{aligned}
\tag{A.15}
$$

which is identical to (A.12).

## APPENDIX B

The mean value and the 95 % confidence interval for the two load internal profiles are shown in Figures B-1 and B-2 for the entire simulation. (Mean value +/- 1.96 times standard deviation assuming a Gaussian distribution)

The external climate is shared with respect to the external air temperature; see Figure 3 in text, whereas the solar radiation depends on the orientation of the windows. The Zone I facade faces north and the Zone II facade faces south. Mean value processes and standard deviation processes for the external temperature as well as the solar radiation (direct and diffuse) are modelled by means of time series analysis of the Danish Design Reference Year (DRY), see [15], as explained in Brohus et al. [16]. The external air temperature for the week in question is shown in Figure B-3 as the mean value and the 95 % confidence interval.

The solar heat gain depends on the type of glass, shading factors, window orientation etc., and is given as a function of the direct and the diffuse solar radiation. A probabilistic model for the solar heat gain, $\Phi_{sun}$, is also presented in [16]. Figures B-4 and B-5 show the mean value and the corresponding 95 % confidence intervals for the two zones.

In Figure B-4, the second peak of the daily solar gain - in the afternoon - is caused by approximations in the model and it is obviously not a physical phenomenon. However, in the present simulations this inaccuracy of the model presumably only has a small influence.

The parameters applied in Test Case 1 are summarised in Table B-1.

The following starting conditions are used

$$E[\theta_i(t=t_0)] = 20 \quad \text{°C}, \quad i = 1, \ldots, 6$$

$$\mathrm{E}[\theta_i(t=t_0)\theta_j(t=t_0)] = 400 \ \text{°C}^2, \quad i = 1, \ldots, 6, \ j = i, \ldots, 6$$

# APPENDIX C

Table C-1 presents the parameters applied in Case Study 2.

An assumed 24-hour load profile for the mean value of the internal sensible heat load is applied in the simulation as shown in Figure C-1. The sensible heat is divided into 50% convective heat, $\Phi_{conv}$, and 50% radiative heat, $\Phi_{rad}$. The convective heat flow is assumed to influence the internal air, i.e. $\theta_1$, and the radiative heat flow is assumed to influence the surface layer, i.e. $\theta_2$.

# APPENDIX D

The specific heat loss due to ventilation can be calculated by;

$$H_{vent} = \rho c_p q \tag{D-1}$$

where $\rho$ is the density, $c_p$ is the specific heat, and $q$ is the volumetric air flow rate. It has been chosen to implement a simple model for stack-driven natural ventilation, $q$.

If we have two columns of air with different densities, see Figure D-1, the pressure difference between two openings, $\Delta p$, separated by a vertical distance of $\Delta h$ is found by [20]

$$\Delta p = \Delta\rho g \Delta h = \frac{\rho \Delta\theta}{\theta_{ext} + 273.15} g \Delta h \tag{D-2}$$

where $\Delta p$ *and* $\Delta h$ are the pressure difference and vertical distance between two openings, $\Delta\theta$ is the corresponding temperature difference, which in the present application happens to be the difference between the internal air temperature, $\theta_1$, and the external air temperature, $\theta_{ext}$, see Figure D-1.

The air flow rate through a large opening is given by

$$q = C_D A \left( \frac{2\Delta p}{\rho} \right)^{1/2} = C_D A \left[ 2 g \Delta h \frac{\theta_1 - \theta_{ext}}{\theta_{ext} + 273.15} \right]^{1/2} \tag{D-3}$$

where $C_D$ is the discharge coefficient and $A$ is the opening area. Instead of a single opening the present model has two openings with areas $A_1$ and $A_2$, respectively. The two serial openings can be replaced by means of one "effective" opening with the same discharge coefficient [21]

$$A = \frac{A_1}{\sqrt{1+m}} \tag{D-4}$$

where $A_1$ is the smaller opening. Assuming turbulent flow, $m$ is expressed as

$$m = \left( \frac{A_1}{A_2} \right)^2 \tag{D-5}$$

In the test $A_1$ equals $A_2$. Thus, $m$ equals 1 and

$$H_{vent} = \rho c_p C_D A (g \Delta h)^{1/2} \left[ \frac{\theta_1 - \theta_{ext}}{\theta_{ext} + 273.15} \right]^{1/2} \tag{D-6}$$

**Table B-1** Parameters applied in Test Case 1. Symbols refer to Figure 3.

| Parameter | Unit | Mean value | Standard deviation | Stochastic ? |
|---|---|---|---|---|
| $\theta_1$ - $\theta_6$ | °C | Unknown | Unknown | Yes |
| $\theta_{ext}$ | °C | See Figure B-3 | See Figure B-3 | Yes |
| $\theta_A$ | °C | 20 | 2 | Yes |
| $\theta_B$ | °C | 26 | 2 | Yes |
| $\theta_C$ | °C | 18 | 1 | Yes |
| $C_1$, $C_4$ | J/K | 75,000 | 0 | No |
| $C_2$, $C_5$ | J/K | 1,250,000 | 0 | No |
| $C_3$, $C_6$ | J/K | 3,750,000 | 0 | No |
| $H_{ventI}$, $H_{ventII}$ | W/K | 60 | 15 | Yes |
| $H_{extI}$, $H_{extII}$ | W/K | 15 | 0 | No |
| $H_{1A}$, $H_{4B}$ | W/K | 20 | 0 | No |
| $H_{1C}$, $H_{4C}$ | W/K | 25 | 0 | No |
| $H_{14}$ | W/K | 100 | 30 | Yes |
| $H_{surfI}$, $H_{surfII}$ | W/K | 300 | 0 | No |
| $H_{strucI}$, $H_{strucII}$ | W/K | 1000 | 0 | No |
| $\Phi_{convI}$ | W | See Figure B-1 | See Figure B-1 | Yes |
| $\Phi_{convII}$ | W | See Figure B-2 | See Figure B-2 | Yes |
| $\Phi_{radI}$ | W | See Figure B-1 | See Figure B-1 | Yes |
| $\Phi_{radII}$ | W | See Figure B-2 | See Figure B-2 | Yes |
| $\Phi_{sunI}$ (north) | W | See Figure B-4 | See Figure B-4 | Yes |
| $\Phi_{sunII}$ (south) | W | See Figure B-5 | See Figure B-5 | Yes |

**Table C-1** Parameters applied in Case Study 2. Symbols refer to Figure 7.

| Parameter | Unit | Mean value | Standard deviation | Stochastic |
|---|---|---|---|---|
| $\theta_1$, $\theta_2$, $\theta_3$ | °C | Output | Output | Yes |
| $\theta_{ext}$ , $\Phi_{sun}$ | °C, W | Data from Danish DRY | Data from Danish DRY | Yes |
| $\theta_{adj}$ | °C | 20 | 2 | Yes |
| $C_1$, $C_2$, $C_3$ | J/K | $6{\cdot}10^5$, $1{\cdot}10^7$, $3{\cdot}10^7$ | 0 | No |
| $H_{vent}$ | W/K | Calculated | Calculated | Yes |
| $H_{ext}$ | W/K | 800 | 0 | No |
| $H_{adj}$ | W/K | 150 | 45 | Yes |
| $H_{surf}$ , $H_{struc}$ | W/K | 1400, 4800 | 0 | No |
| $\Phi_{conv}$, $\Phi_{rad}$ | W | Assumed data sets | 0.3 times mean value | Yes |

**Figure 1** Building calculation model with one internal air temperature for each zone, e.g. $\theta_1$, assuming fully mixed conditions. On the surfaces and inside the structures an arbitrary number of nodes are possible, e.g. $\theta_2$ and $\theta_3$. Boundary nodes like the adjacent zone temperature, $\theta_1^b$, and the external temperature, $\theta_2^b$, prescribe the loads together with convective heat flow supplied to the air, e.g. $\Phi_{11}$ and $\Phi_{12}$, and radiation heat flow supplied to surfaces, e.g. $\Phi_{21}$. The unknown nodes are interconnected via specific heat losses, e.g. $H_{12}$ and $H_{23}$, and connected to the boundary nodes via another set of specific heat losses, e.g. $H_{11}^b$ and $H_{12}^b$. The specific heat losses may also include heat transfer due to ventilation. The effective thermal heat capacities, e.g. $C_1$, $C_2$, and $C_3$ are applied as "lumped masses" in the nodes.

**Figure 2** Principle of the Runge-Kutta update. $y_{n+1}$ is calculated using $y_n$ from the previous time step and the intermediate points 2-3. The dashed line represents the "true" solution and the short solid lines the derivatives at $y_n$ and the intermediate points.

**Figure 3** Case Study 1 building model: Two zones surrounded by three adjacent zones and the external climate. The external temperature, $\theta_{ext}$, is shared by Zone I and Zone II.

**Figure 4** Internal air temperature mean value in Zone I, $\theta_1$, (dark colour) and internal air temperature mean value in Zone II, $\theta_4$, (light colour) both for Test Case 1.

**Figure 5** Internal air temperature in Zone I, $\theta_1$, and surface layer temperature in Zone I, $\theta_2$, both for Test Case 1. The figure shows the mean values (dark colour) and the 95% confidence intervals (light colour).

**Figure 6** Three stochastic realisations (thin lines) of internal air temperature in Zone I, $\theta_1$, and surface layer temperature in Zone I, $\theta_2$, both for Test Case 1. The figure also shows the 95% confidence intervals (thick light lines). In order to illustrate the stochastic fluctuations clearly the plot is limited to show the first 5.5 hours of the week.

**Figure 7** Case Study 2. An atrium surrounded by an adjacent zone and the external climate. Three unknown temperatures are to be determined, i.e. $\theta_1$ - $\theta_3$. The surface-layer accounts for one-fourth of the building thermal mass and the "structure" accounts for the rest.

**Figure 8** Methods for coupling of thermal models and air flow models (adapted from Orme, 1999). When the governing equations for heat transfer and air flow are solved simultaneously, the method of coupling may be termed "full integration".

**Figure 9** Internal air temperature in the atrium, $\theta_1$, for a week during winter (left) and during summer (right). The figure shows the mean value (dark colour) and the 95% confidence interval (light colour).

**Figure 10** Mean air change rate (dark colour) and standard deviation (light colour) during a winter week (left) and a summer week (right).

**Figure A.1** Two realisations of a standard Wiener process.

**Figure B-1** Load profile for internal sensible heat Zone I. The mean value (dark colour) and the 95% confidence interval (light colour) are shown.

**Figure B-2** Load profile for internal sensible heat Zone II. The mean value (dark colour) and the 95% confidence interval (light colour) are shown.

**Figure B-3** External air temperature applied during the simulations in Test Case 1. The mean value (dark colour) and the 95% confidence interval (light colour) are shown.

**Figure B-4** Solar heat gain in Zone I where the facade faces north. The mean value (dark colour) and the 95% confidence interval (light colour) are shown.

**Figure B-5** Solar heat gain in Zone II where the facade faces south. The mean value (dark colour) and the 95% confidence interval (light colour) are shown.

**Figure C-1** Load profiles for internal sensible heat. The mean value (dark colour) and the 95% confidence interval (light colour) are shown.

**Figure D-1** Natural ventilated atrium with two openings.

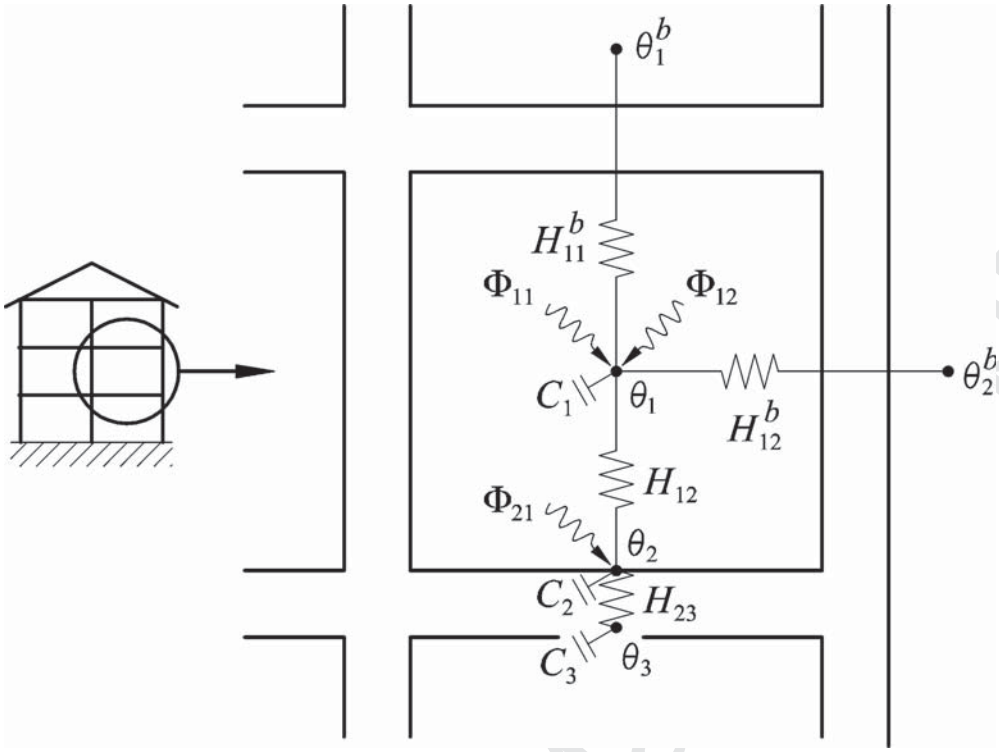


**Figure 1** Building calculation model with one internal air temperature for each zone, e.g. $\theta_1$, assuming fully mixed conditions. On the surfaces and inside the structures an arbitrary number of nodes are possible, e.g. $\theta_2$ and $\theta_3$. Boundary nodes like the adjacent zone temperature, $\theta_1^b$, and the external temperature, $\theta_2^b$, prescribe the loads together with convective heat flow supplied to the air, e.g. $\Phi_{11}$ and $\Phi_{12}$, and radiation heat flow supplied to surfaces, e.g. $\Phi_{21}$. The unknown nodes are interconnected via specific heat losses, e.g. $H_{12}$ and $H_{23}$, and connected to the boundary nodes via another set of specific heat losses, e.g. $H_{11}^b$ and $H_{12}^b$. The specific heat losses may also include heat transfer due to ventilation. The effective thermal heat capacities, e.g. $C_1$, $C_2$, and $C_3$ are applied as "lumped masses" in the nodes.

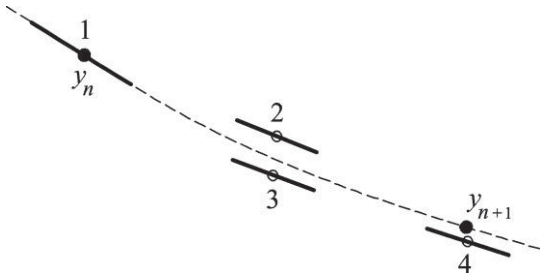


**Figure 2** Principle of the Runge-Kutta update. $y_{n+1}$ is calculated using $y_n$ from the previous time step and the intermediate points 2-3. The dashed line represents the "true" solution and the short solid lines the derivatives at $y_n$ and the intermediate points.

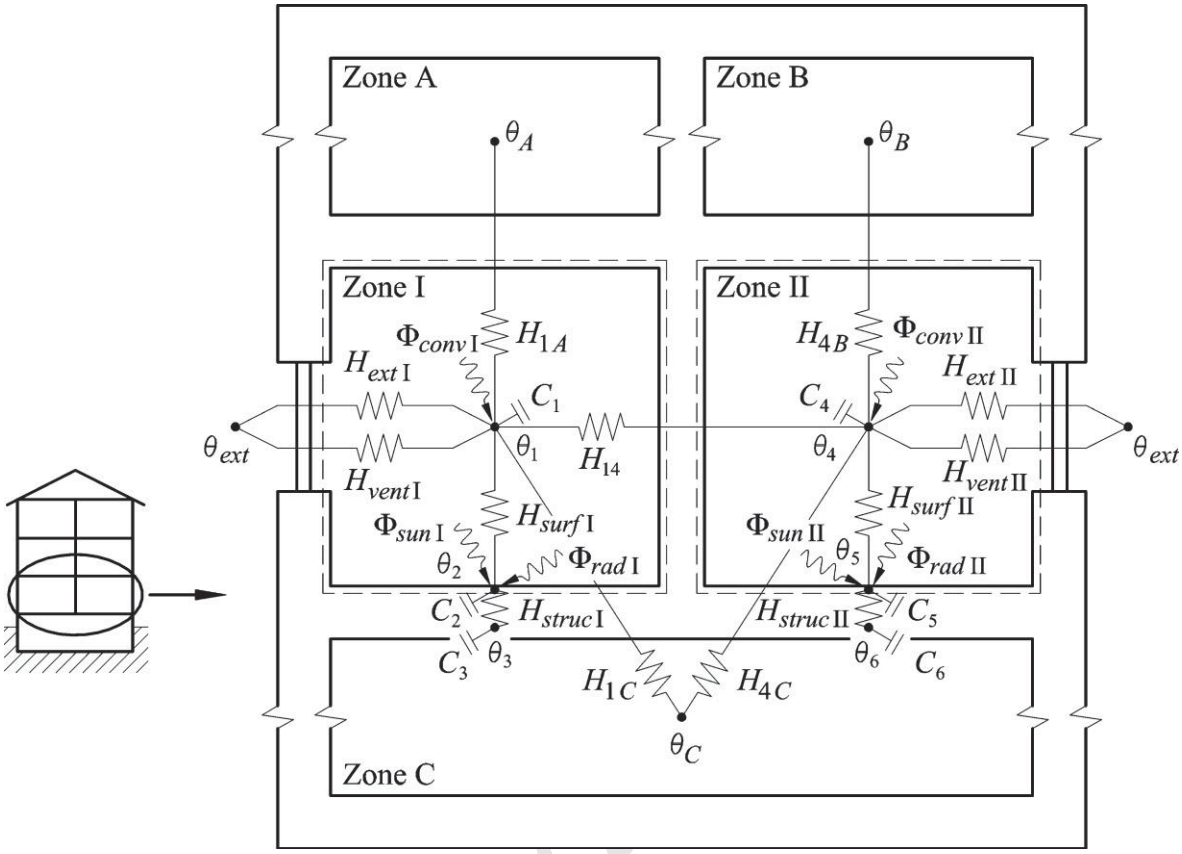


**Figure 3** Case Study 1 building model: Two zones surrounded by three adjacent zones and the external climate. The external temperature, $\theta_{ext}$, is shared by Zone I and Zone II.

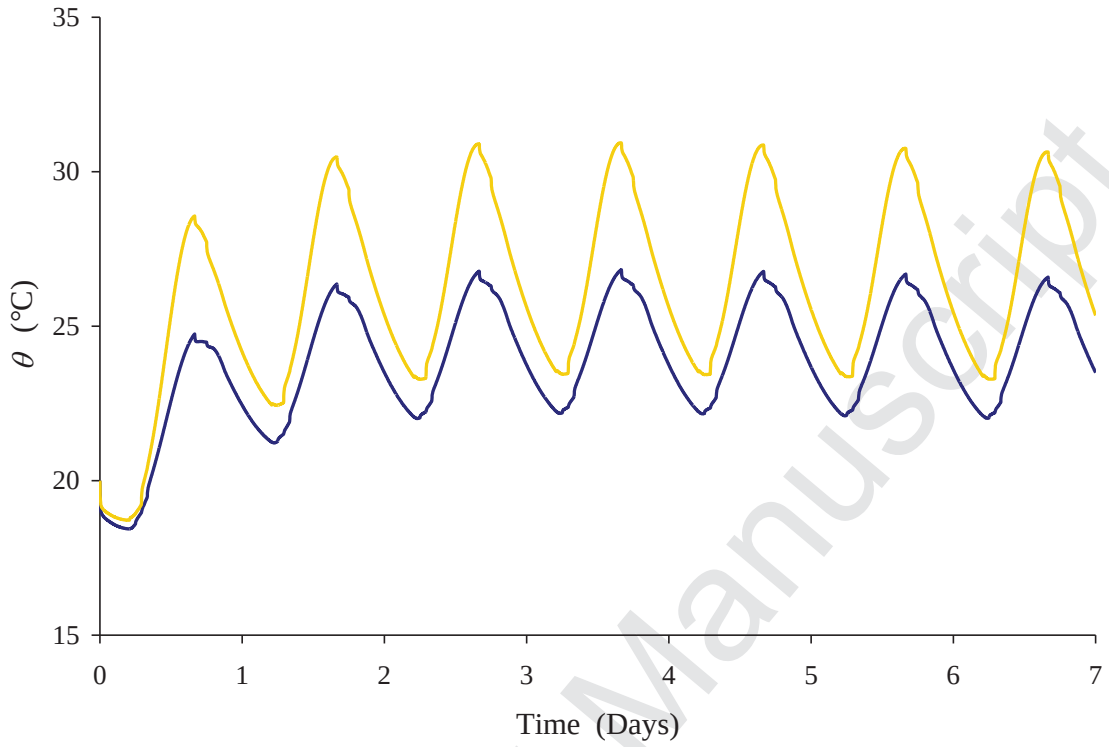


**Figure 4** Internal air temperature mean value in Zone I, $\theta_1$, (dark colour) and internal air temperature mean value in Zone II, $\theta_4$, (light colour) both for Test Case 1.

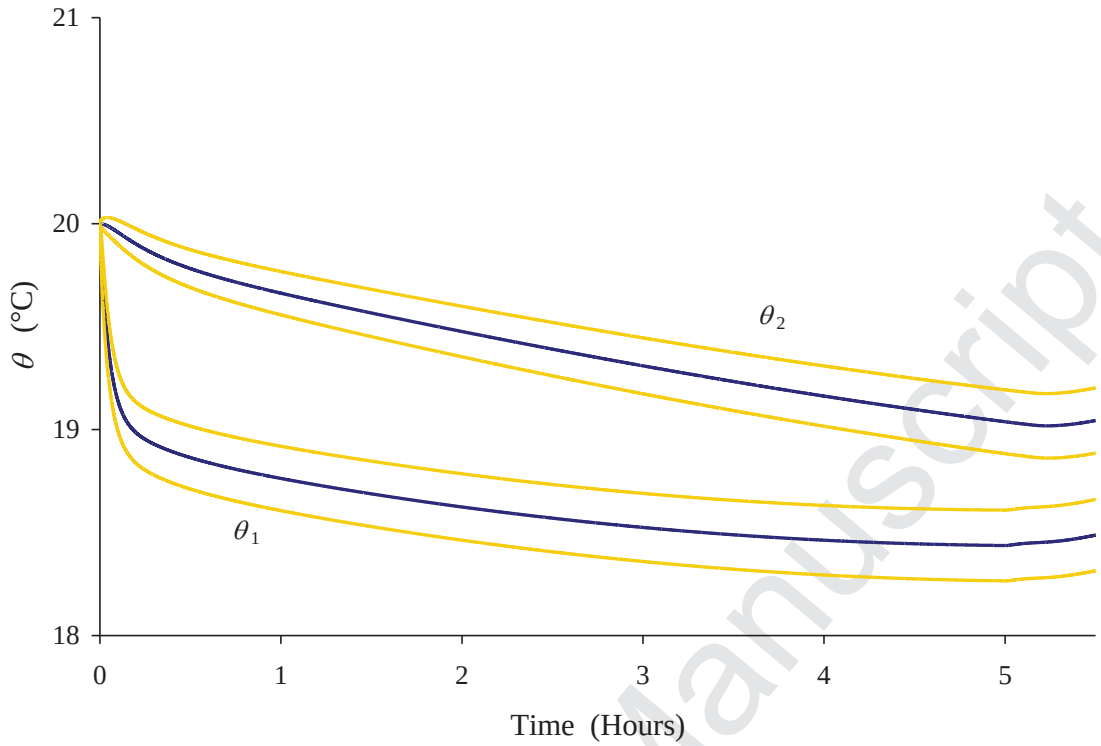


**Figure 5** Internal air temperature in Zone I, $\theta_1$, and surface layer temperature in Zone I, $\theta_2$, both for Test Case 1. The figure shows the mean values (dark colour) and the 95% confidence intervals (light colour).

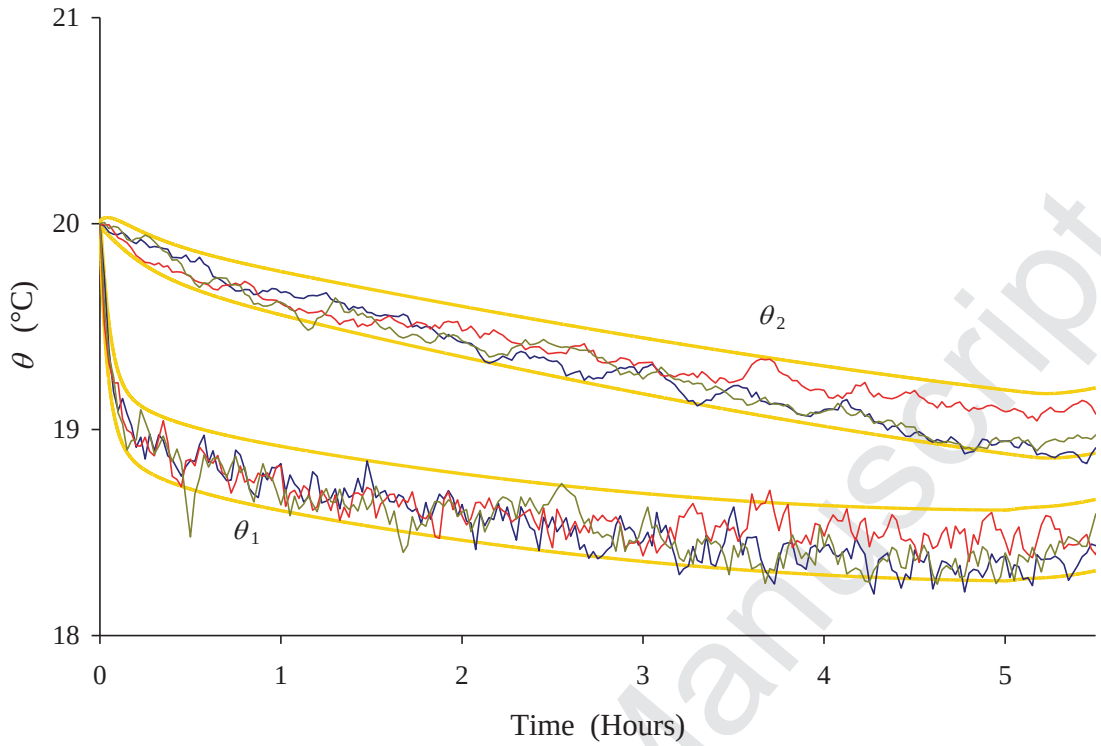


**Figure 6** Three stochastic realisations (thin lines) of internal air temperature in Zone I, $\theta_1$, and surface layer temperature in Zone I, $\theta_2$, both for Test Case 1. The figure also shows the 95% confidence intervals (thick light lines). In order to illustrate the stochastic fluctuations clearly the plot is limited to show the first 5.5 hours of the week.

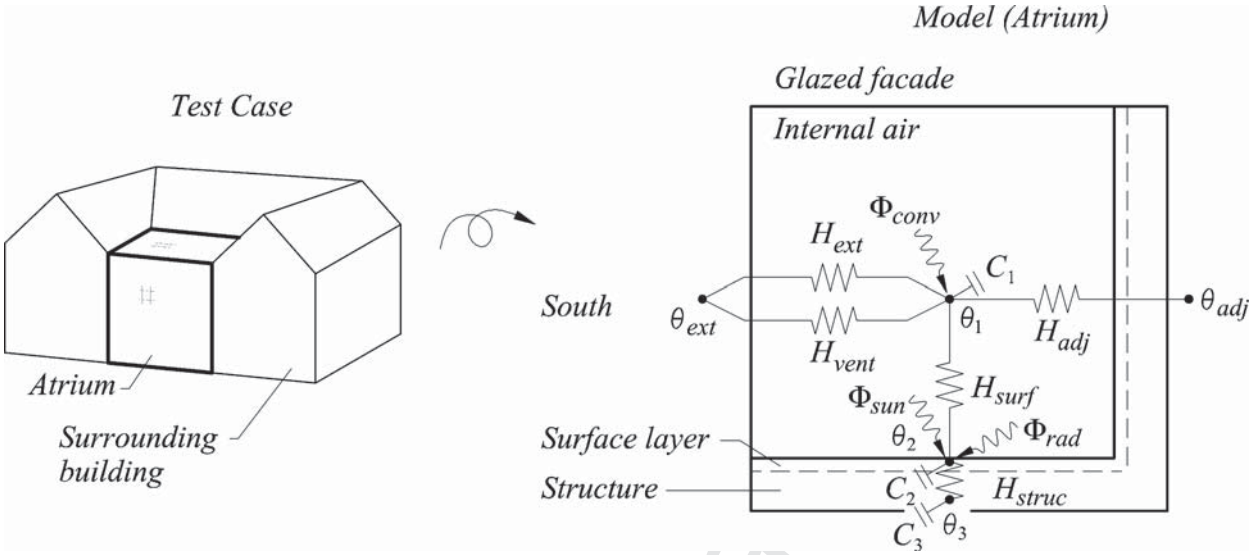


**Figure 7** Case Study 2. An atrium surrounded by an adjacent zone and the external climate. Three unknown temperatures are to be determined, i.e. $\theta_1$ - $\theta_3$. The surface-layer accounts for one-fourth of the building thermal mass and the "structure" accounts for the rest.

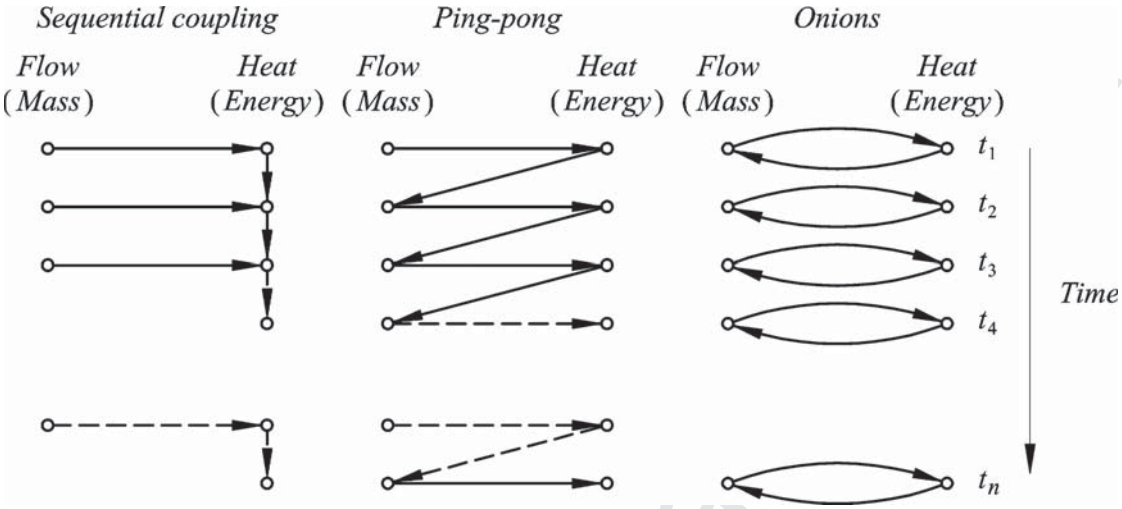


**Figure 8** Methods for coupling of thermal models and air flow models (adapted from Orme, 1999). When the governing equations for heat transfer and air flow are solved simultaneously, the method of coupling may be termed "full integration".

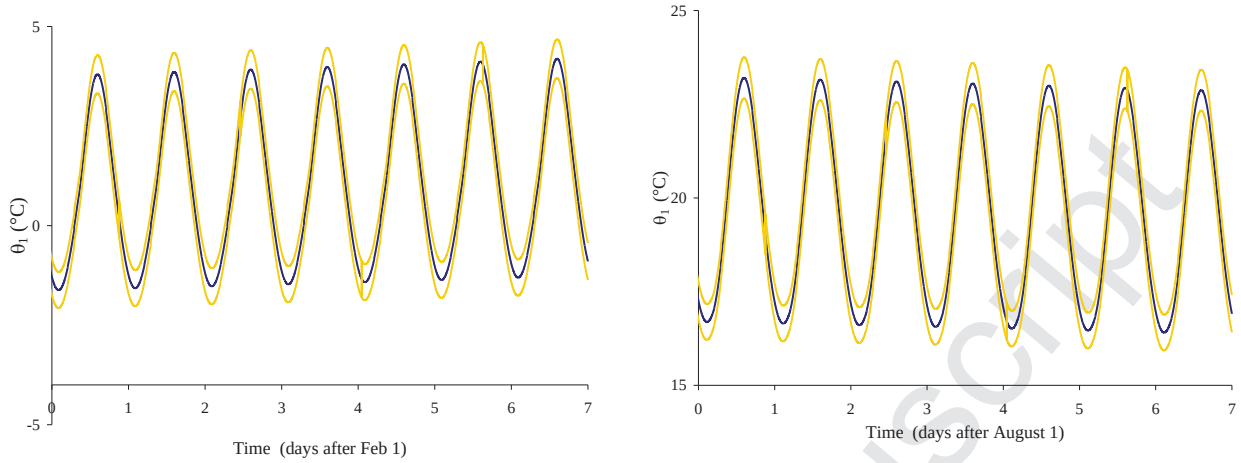


**Figure 9** Internal air temperature in the atrium, $\theta_1$, for a week during winter (left) and during summer (right). The figure shows the mean value (dark colour) and the 95% confidence interval (light colour).

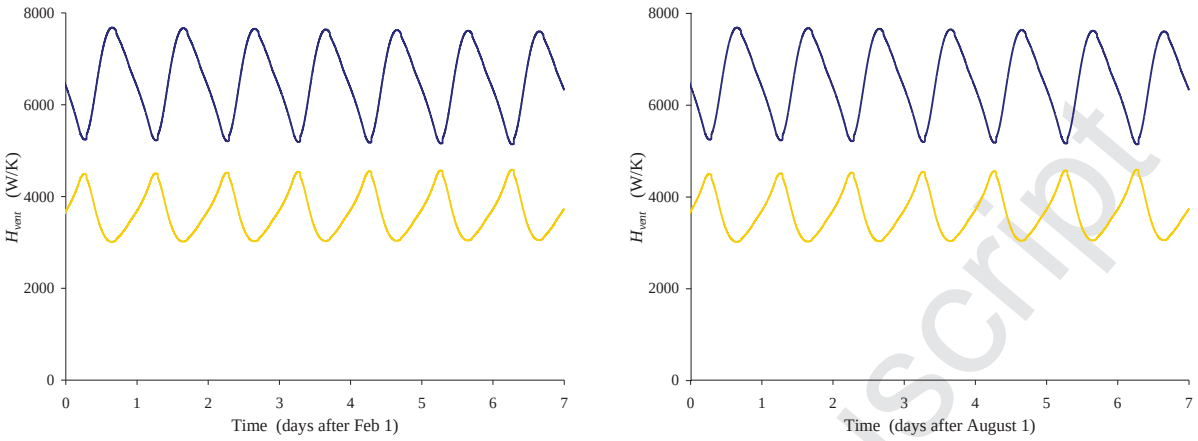


**Figure 10** Mean air change rate (dark colour) and standard deviation (light colour) during a winter week (left) and a summer week (right).

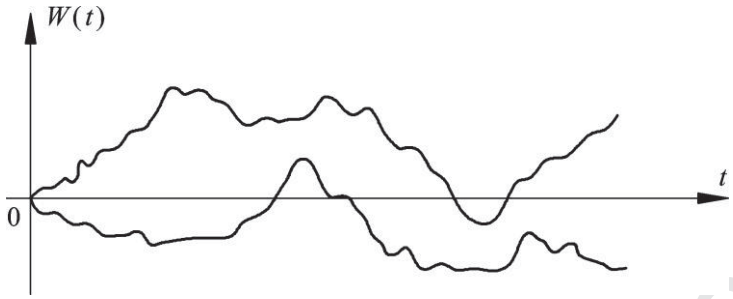


**Figure A.1** Two realisations of a standard Wiener process.

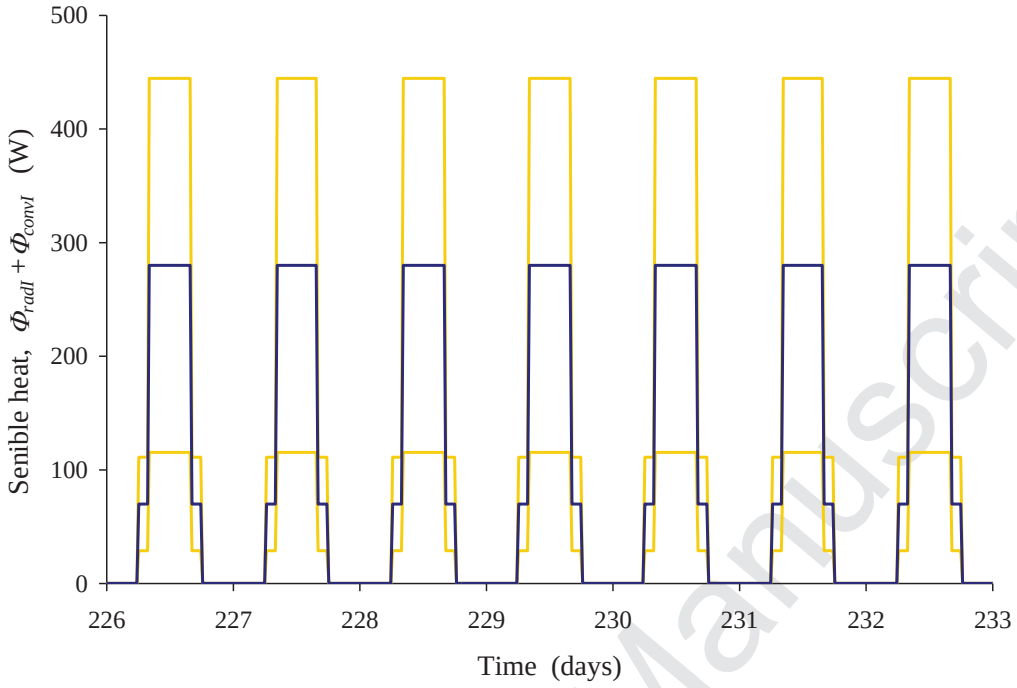


**Figure B-1** Load profile for internal sensible heat Zone I. The mean value (dark colour) and the 95% confidence interval (light colour) are shown.

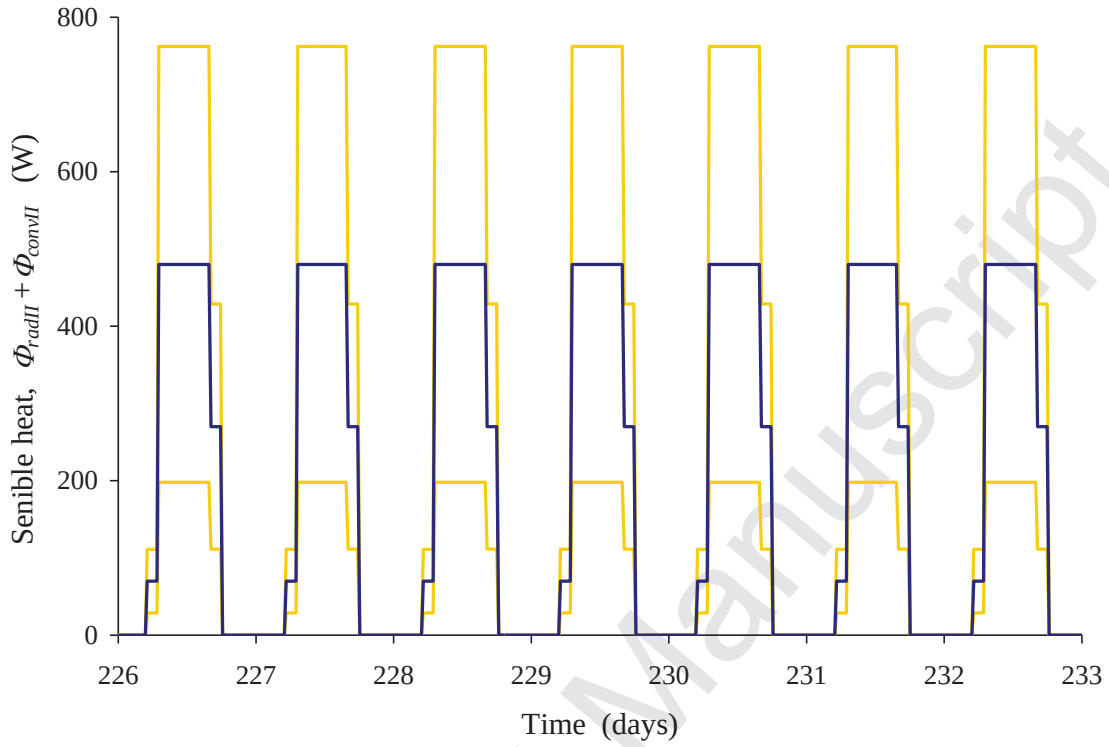


**Figure B-2** Load profile for internal sensible heat Zone II. The mean value (dark colour) and the 95% confidence interval (light colour) are shown.

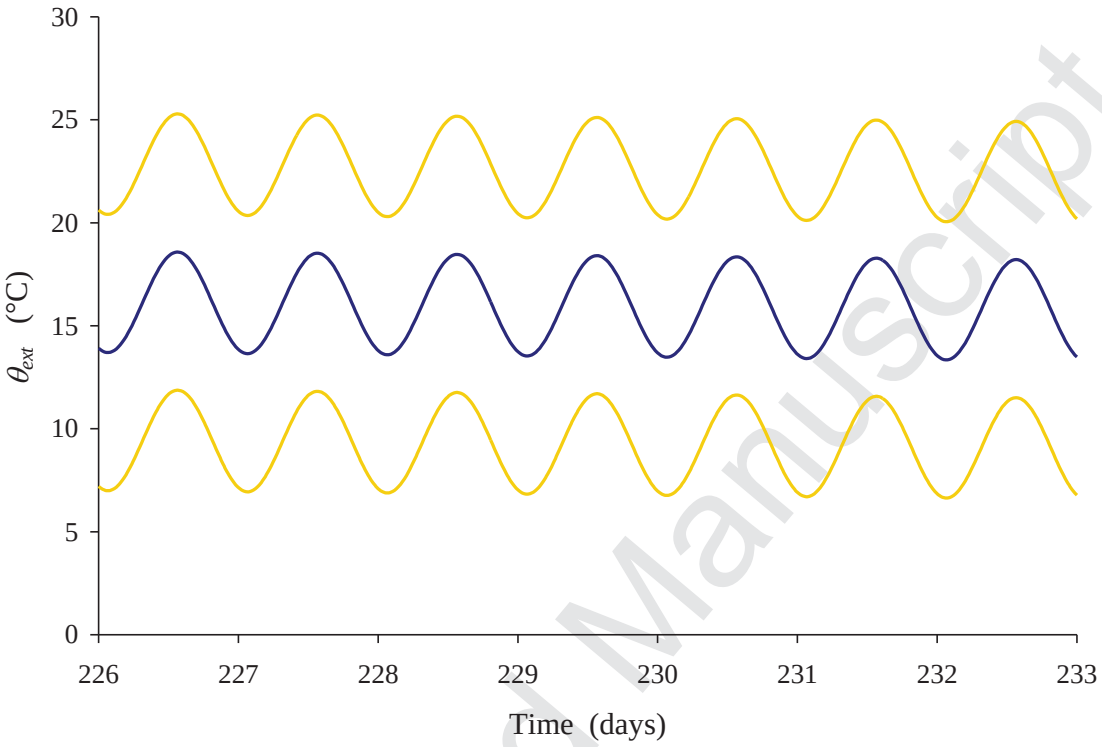


**Figure B-3** External air temperature applied during the simulations in Test Case 1. The mean value (dark colour) and the 95% confidence interval (light colour) are shown.

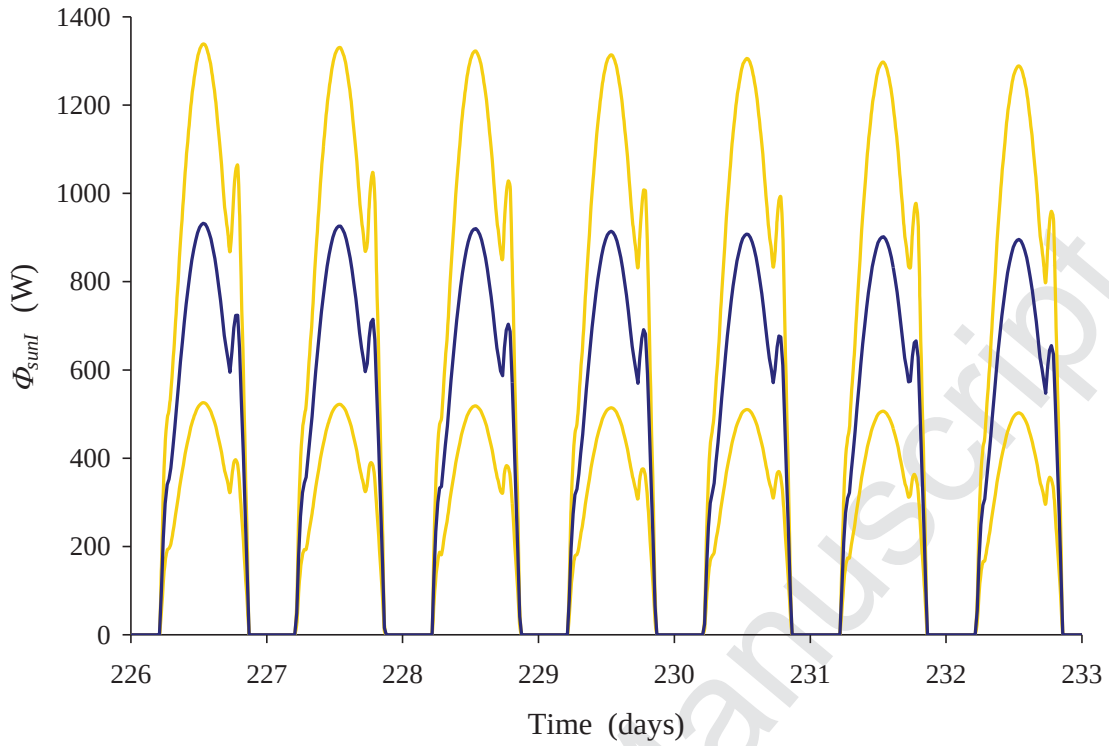


**Figure B-4** Solar heat gain in Zone I where the facade faces north. The mean value (dark colour) and the 95% confidence interval (light colour) are shown.

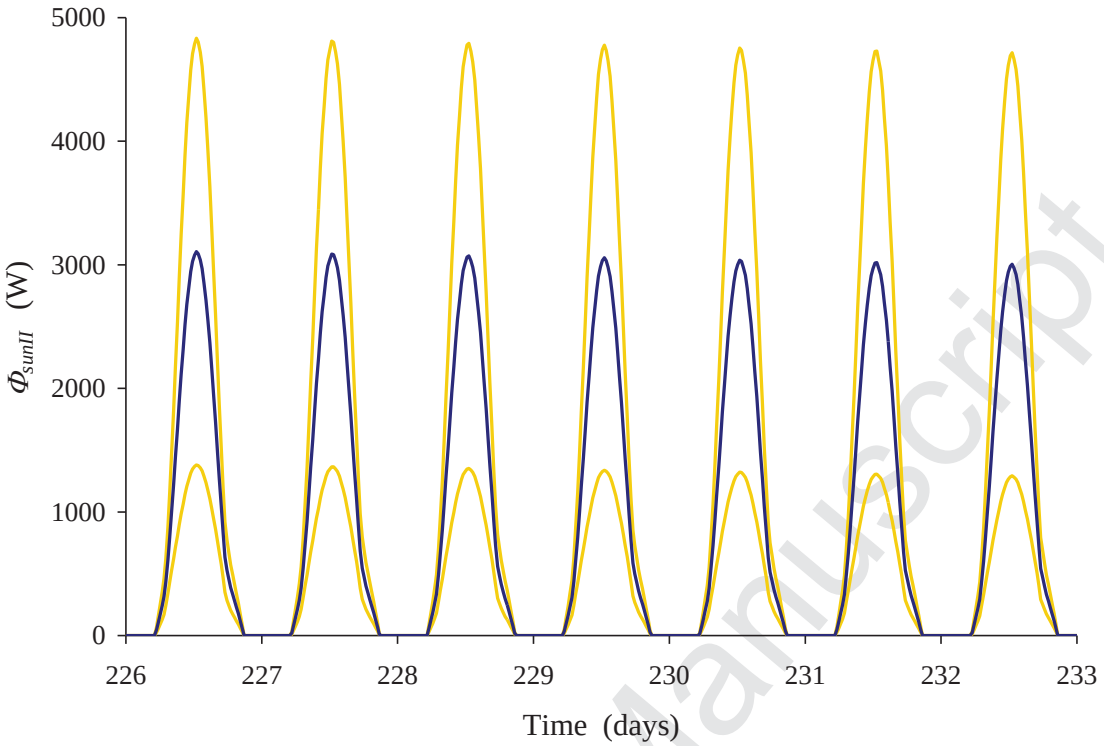


**Figure B-5** Solar heat gain in Zone II where the facade faces south. The mean value (dark colour) and the 95% confidence interval (light colour) are shown.

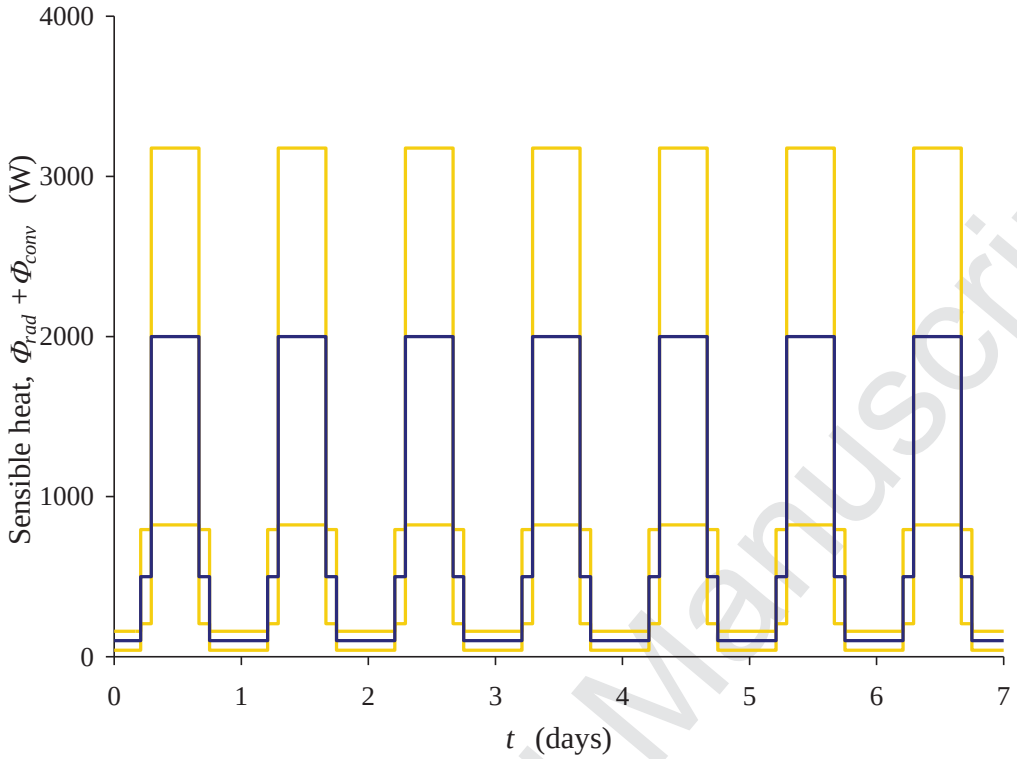


**Figure C-1** Load profiles for internal sensible heat. The mean value (dark colour) and the 95% confidence interval (light colour) are shown.

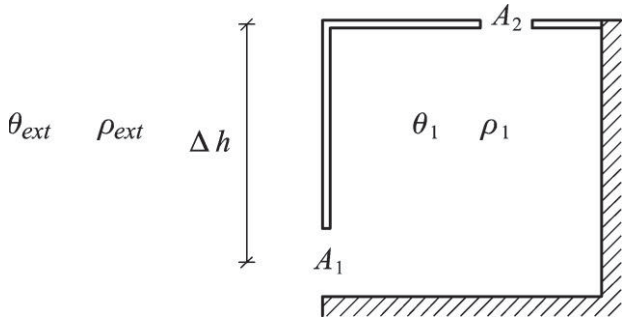


**Figure D-1** Natural ventilated atrium with two openings.

- New approach to improved prediction of building energy consumption
- Quantification of uncertainty using stochastic differential equations
- Determination of the mean value process and the standard deviation process
- Probabilistic method providing uncertainty variation as a function of time